Caos em Equações Diferenciais

Referência Principal: *Chaos*

K. Alligood, T. D. Sauer, J. A. Yorke

Springer (1997)

Convecção em um gradiente de temperatura

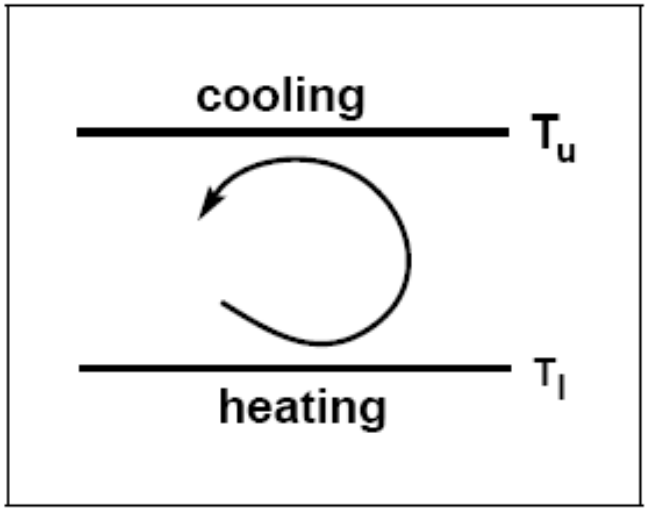

Figure 9.1 Rayleigh-Bénard convection.
The way in which heat rises in a fluid from the lower warm plate to the higher cool plate depends on the temperature difference $T_u - T_l$ of the plates. If the difference is small, heat is transferred by conduction. For a larger difference, the fluid itself moves, in convection rolls.

Chaos
Alligood et al.

Sistema de Lorenz

$$\dot{x} = -\sigma x + \sigma y$$

$$\dot{y} = -x y + r x - y$$

$$\dot{z} = x y - b z$$

Variáveis: $x, y, z \rightarrow$ espaço de fase tridimensional

Parâmetros de controle: σ, r, b

Atrator Caótico
Sistema de Lorenz

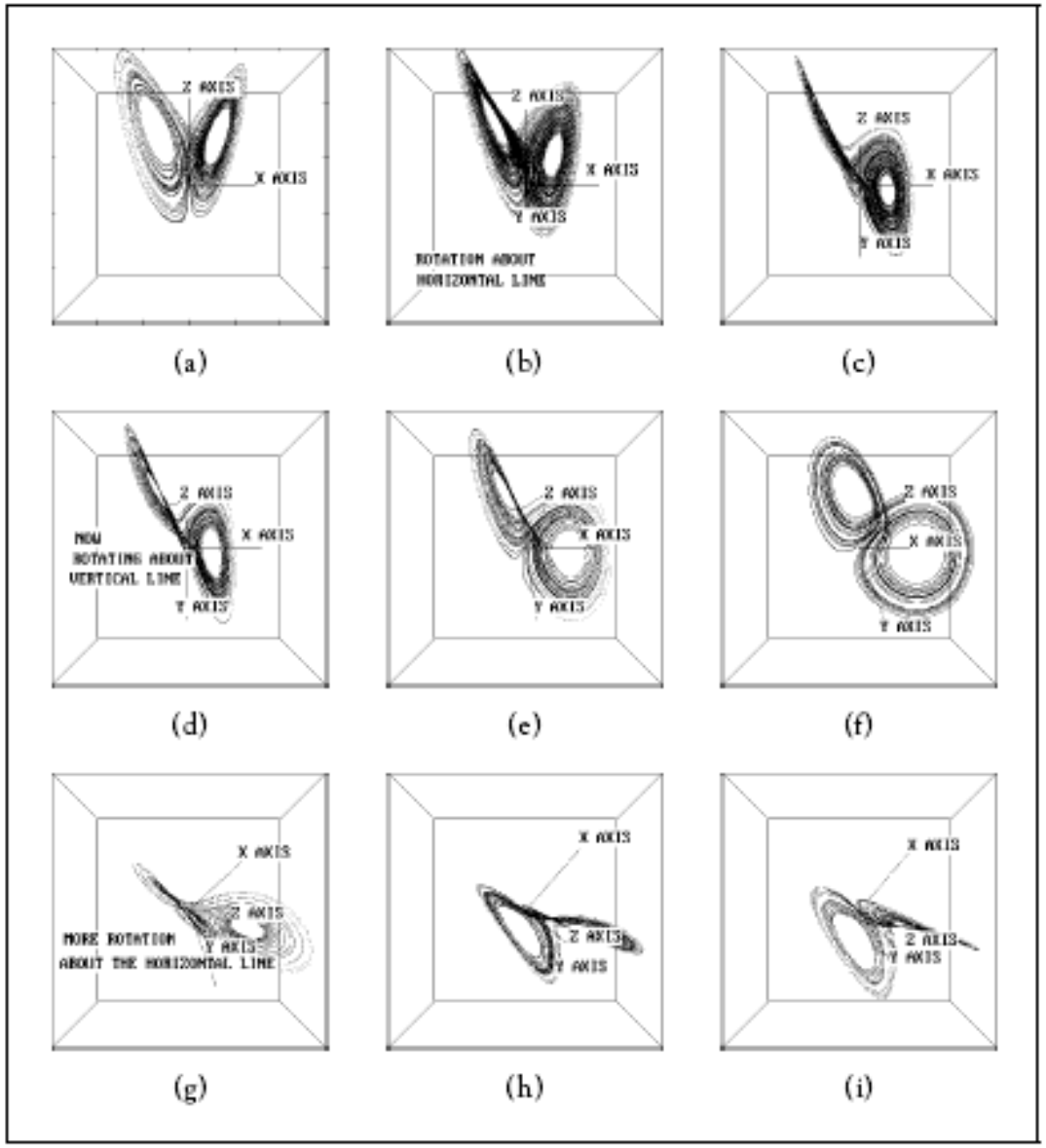

Figure 9.2 Several rotated views of the Lorenz attractor with $r = 28$.
In frames (a)–(c), the attractor is tipped up (rotated about the horizontal x-axis) until the left lobe is edge-on. In frames (d)–(f), the attractor is rotated to the left, around a vertical line. In frames (g)–(i), more rotation about a horizontal line.

Chaos
Alligood et al.

Ampliação do Atrator de Lorenz

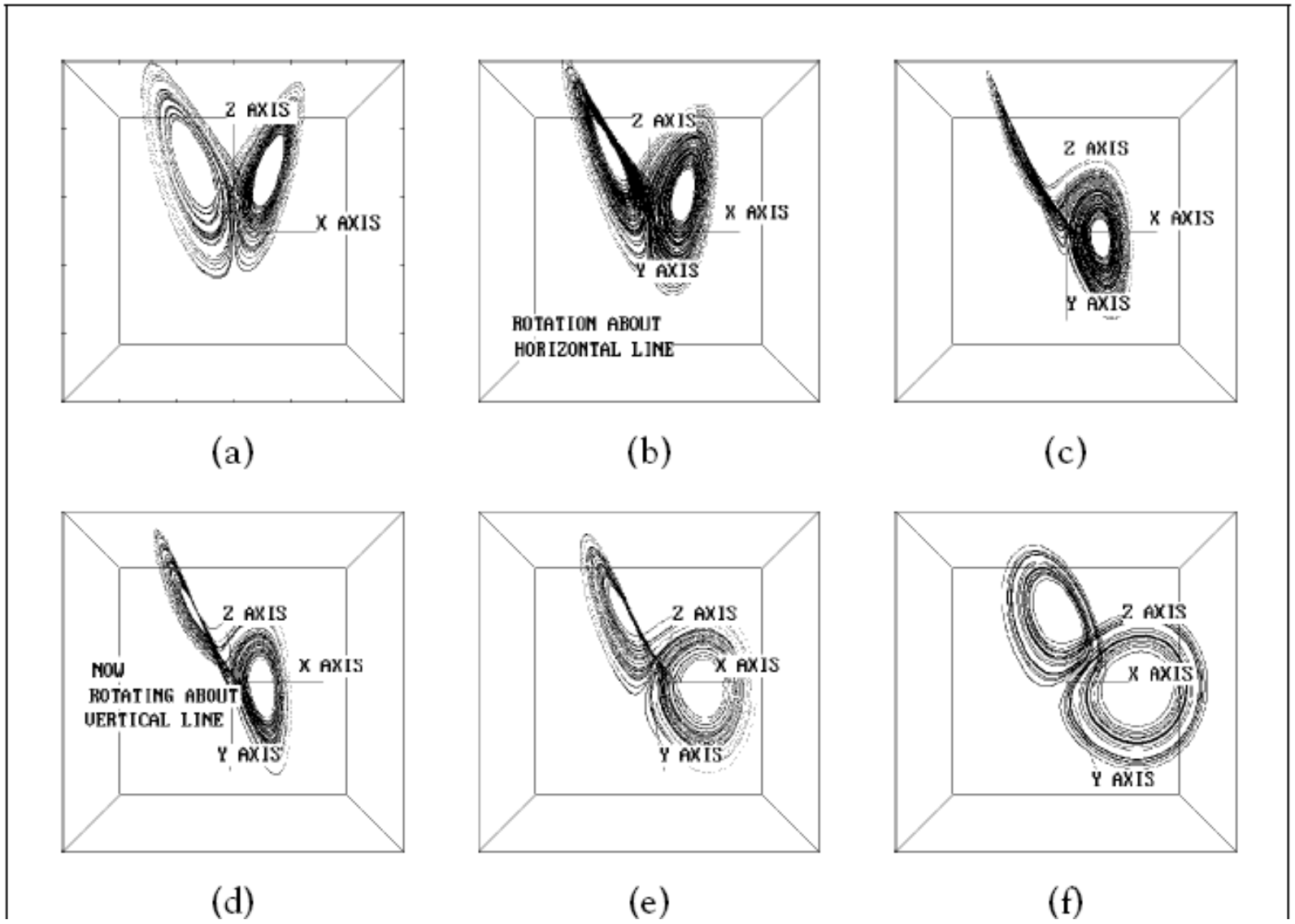

Ampliação do Atrator de Lorenz

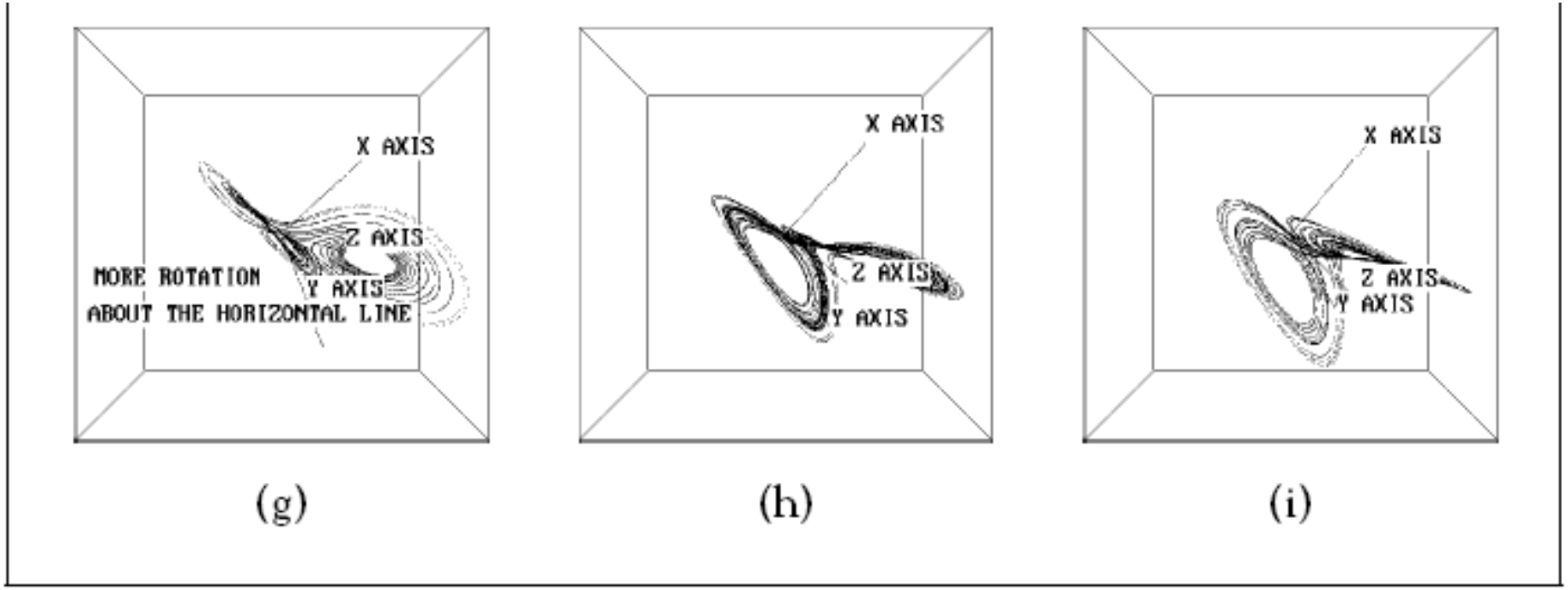

Figure 9.2 Several rotated views of the Lorenz attractor with $r = 28$. In frames (a)–(c), the attractor is tipped up (rotated about the horizontal x-axis) until the left lobe is edge-on. In frames (d)–(f), the attractor is rotated to the left, around a vertical line. In frames (g)–(i), more rotation about a horizontal line.

Sistema de Lorenz

$$\dot{x} = -\sigma x + \sigma y$$

$$\dot{y} = -x y + r x - y$$

$$\dot{z} = x y - b z$$

Variáveis: $x, y, z \rightarrow$ espaço de fase tridimensional

Parâmetros de controle: σ, r, b

Atratores do Sistema de Lorenz

r	Attractor
$[-\infty, 1.00]$	$(0, 0, 0)$ is an attracting equilibrium
$[1.00, 13.93]$	C_+ and C_- are attracting equilibria; the origin is unstable
$[13.93, 24.06]$	Transient chaos: There are chaotic orbits but no chaotic attractors
$[24.06, 24.74]$	A chaotic attractor coexists with attracting equilibria C_+ and C_-
$[24.74, ?]$	Chaos: Chaotic attractor exists but C_+ and C_- are no longer attracting

Table 9.1 Attractors for the Lorenz system (9.1).
For $\sigma = 10$, $b = 8/3$, a wide range of phenomena occur as r is varied.

Chaos
Alligood et al.

Pontos fixos:

$O \equiv (x,\ y,\ z) = (0, 0, 0)$

$C \equiv (\sqrt{b\,(r-1)},\ \sqrt{b\,(r-1)},\ r-1)$

$C' \equiv (-\sqrt{b\,(r-1)},\ -\sqrt{b\,(r-1)},\ r-1)$

$b = 8/3 \quad \sigma = 10 \quad r > 0$

Estabilidade do ponto O é determinada pelos auto-valores λ da matriz jacobiana

$$\begin{bmatrix} -\sigma-\lambda & \sigma & 0 \\ r & -1-\lambda & 0 \\ 0 & 0 & -b-\lambda \end{bmatrix} = 0$$

Ponto O estável no intervalo $0 < r < 1$, pois $\lambda_i < 0$

$r > 1 \Rightarrow$ Ponto O instável $\begin{cases} \lambda_1 > 0 & \Rightarrow \text{variedade instável unidimensional} \\ \lambda_{2,3} < 0 & \Rightarrow \text{variedade estável bidimensional} \end{cases}$

$r_s > r > 1 \Rightarrow$ Pontos C e C′ estáveis, $\lambda_{1,2,3}$ reais

$r_s > r > 1$

C e C′ atratores

Bacias atração separadas pela variedade bidimensional estável do ponto O

$r_0 > r > r_s$

$\lambda_{1,2}$ *complexos*, $\mathrm{Re}\lambda_{1,2} < 0$

C e C′ atratores

$r = r_o = 13.93 \Rightarrow$ Órbitas homoclínicas

$$r > r_0 = 13.93 \Rightarrow \textit{caos transiente e caos} \begin{cases} r < 24.06 \Rightarrow \textit{transiente caótico} \\ r > 24.06 \Rightarrow \textit{atrator caótico} \\ (\textit{coexiste com atratores } C \textit{ e } C') \\ r > 24.74 \Rightarrow \text{C e C}' \textit{ pontos de sela} \\ (\textit{atrator caótico persiste}) \end{cases}$$

Origem do Atrator Caótico de Lorenz

a) O ponto fixo estável
b) O instável; C, C` estáveis
c) O instável, C, C` estáveis
d) Idem
e) Órbita homoclínica
f) Atrator caótico

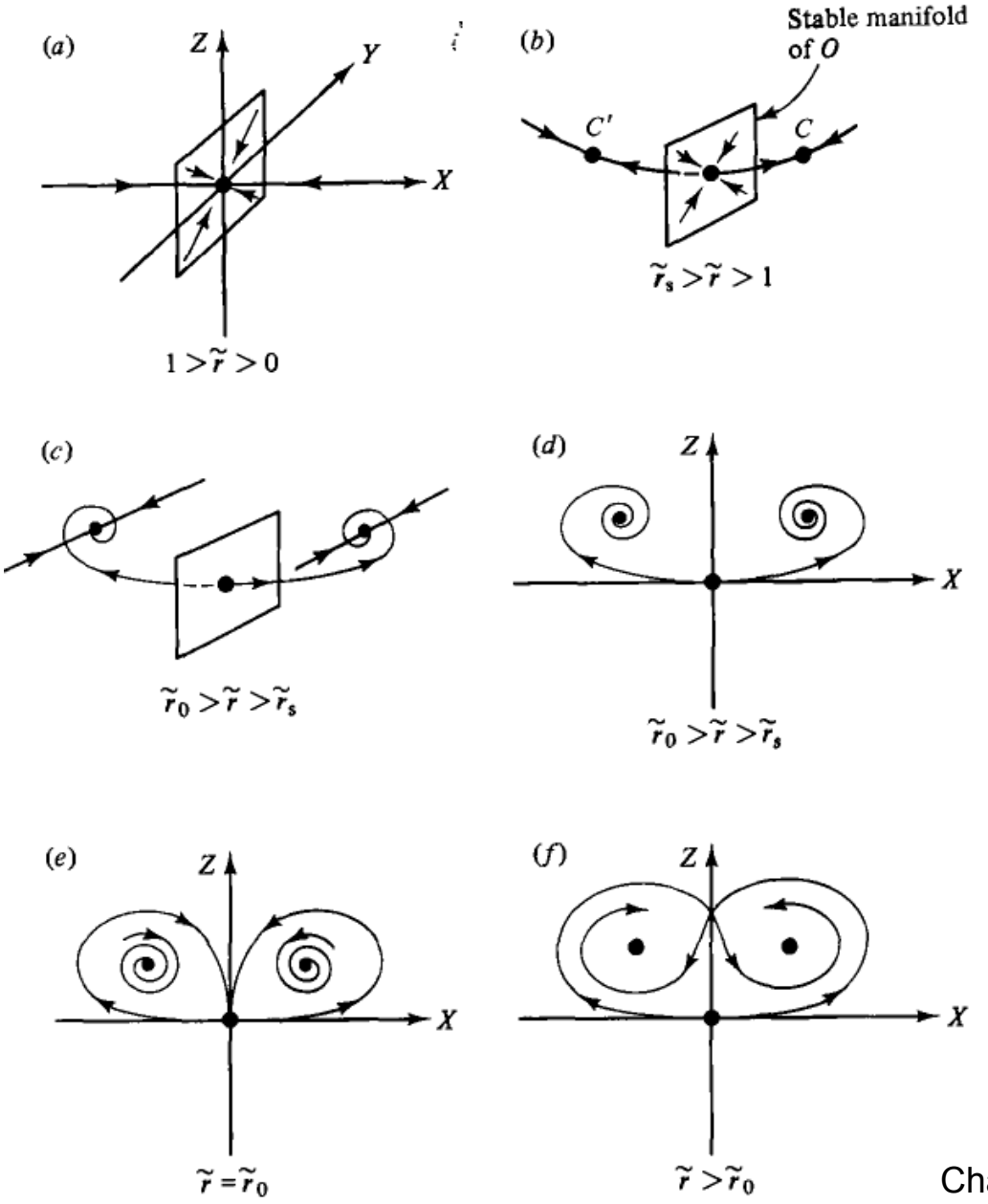

Chaos
Ott

Atratores do Sistema de Lorenz

r	Attractor
$[-\infty, 1.00]$	$(0, 0, 0)$ is an attracting equilibrium
$[1.00, 13.93]$	C_+ and C_- are attracting equilibria; the origin is unstable
$[13.93, 24.06]$	Transient chaos: There are chaotic orbits but no chaotic attractors
$[24.06, 24.74]$	A chaotic attractor coexists with attracting equilibria C_+ and C_-
$[24.74, ?]$	Chaos: Chaotic attractor exists but C_+ and C_- are no longer attracting

Table 9.1 Attractors for the Lorenz system (9.1).
For $\sigma = 10$, $b = 8/3$, a wide range of phenomena occur as r is varied.

Chaos
Alligood et al.

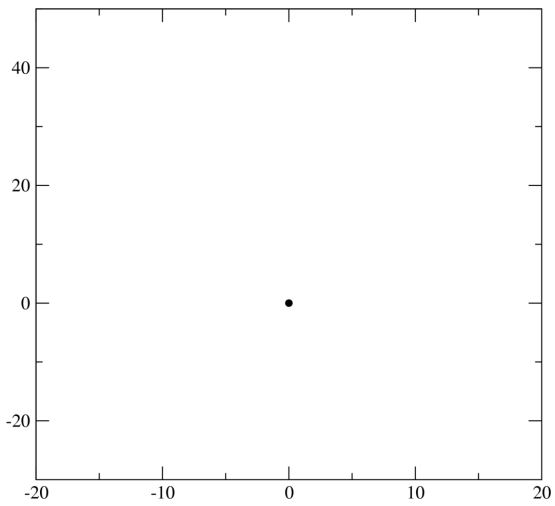

Figura 1 – Para $r = 0$, a origem é ponto fixo estável

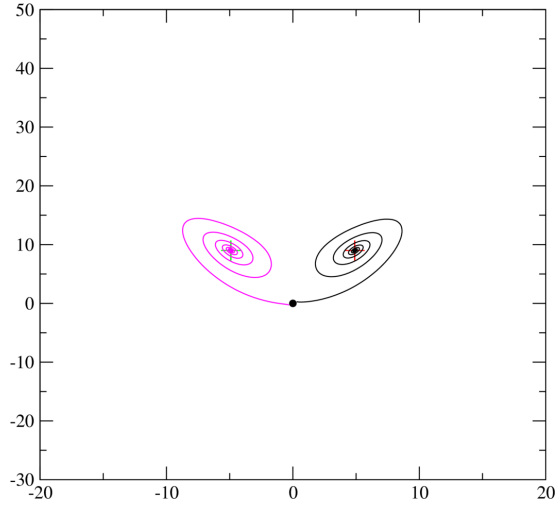

Figura 2 – Para $r = 10$, a origem é ponto fixo instável e surgem dois outros pontos fixos estáveis C_+ e C_-

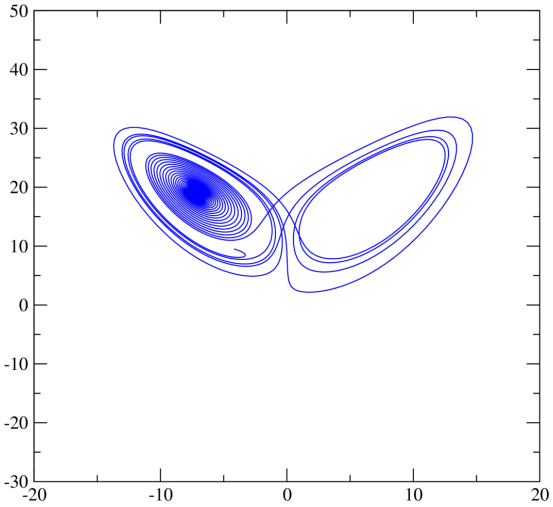

Figura 3 – Para $r = 20$, existem órbitas caóticas não atratoras (transientes)

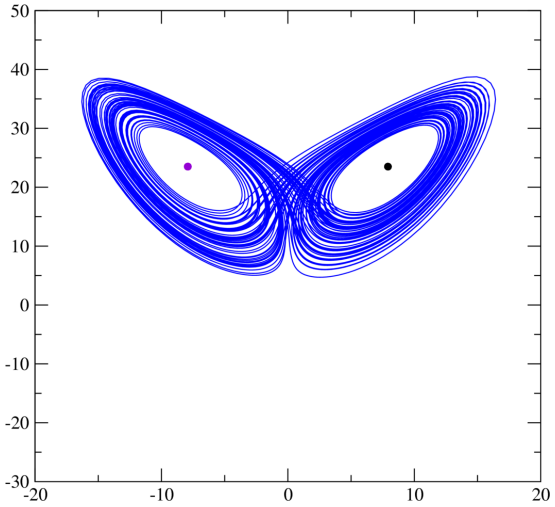

Figura 4 – Para $r = 24.5$, coexistência do atrator caótico com os pontos fixos estáveis C_+ e C_-

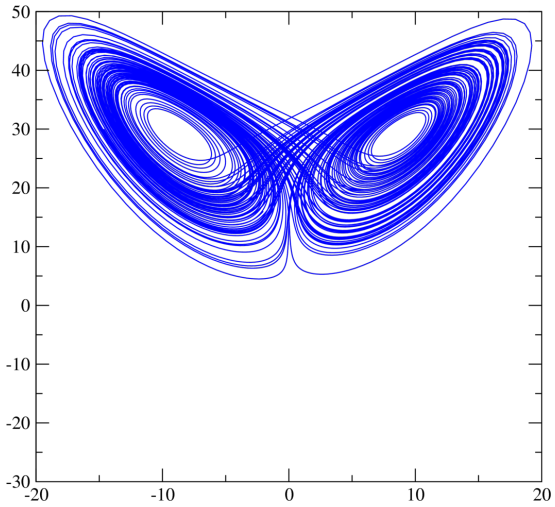

Figura 5 – Para $r = 30$, só existe o atrator caótico

Mapa de Retorno do Atrator de Lorenz

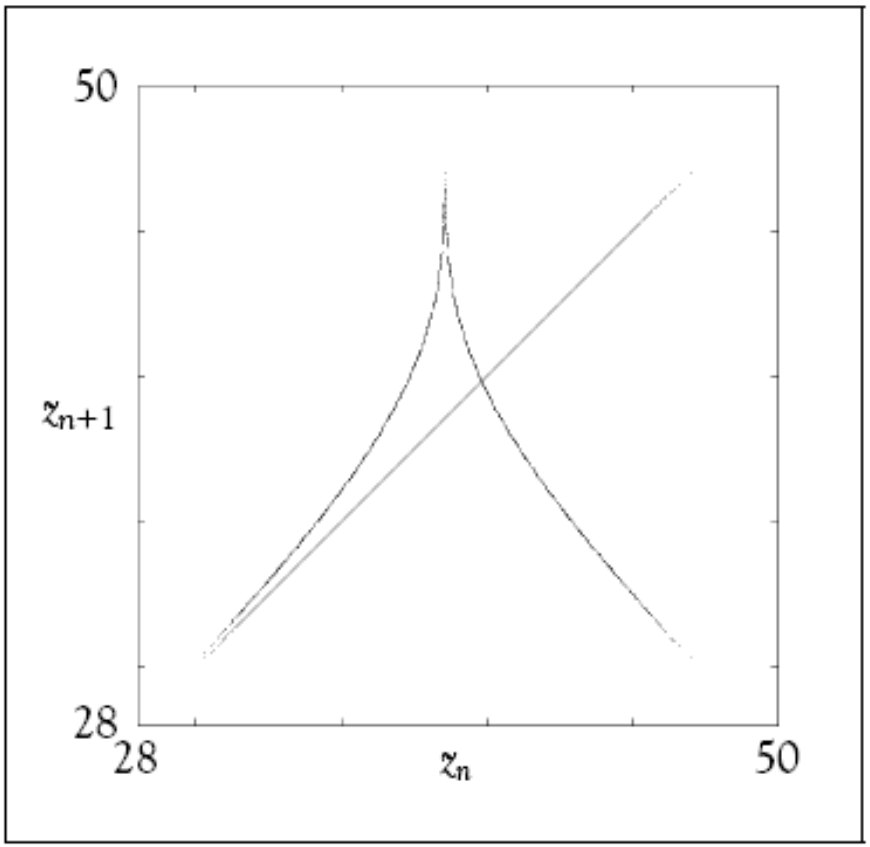

Figure 9.3 Successive maxima of z-coordinate of Lorenz attractor.
Each plotted dot on the tent-like map is a pair (z_n, z_{n+1}) of maximum z-coordinates of loops of the trajectory, one following the other. The nearly one-dimensional nature of the map arises from the very strong volume contraction.

Chaos
Alligood et al.

Diagrama de Bifurcação para o Sistema de Lorenz

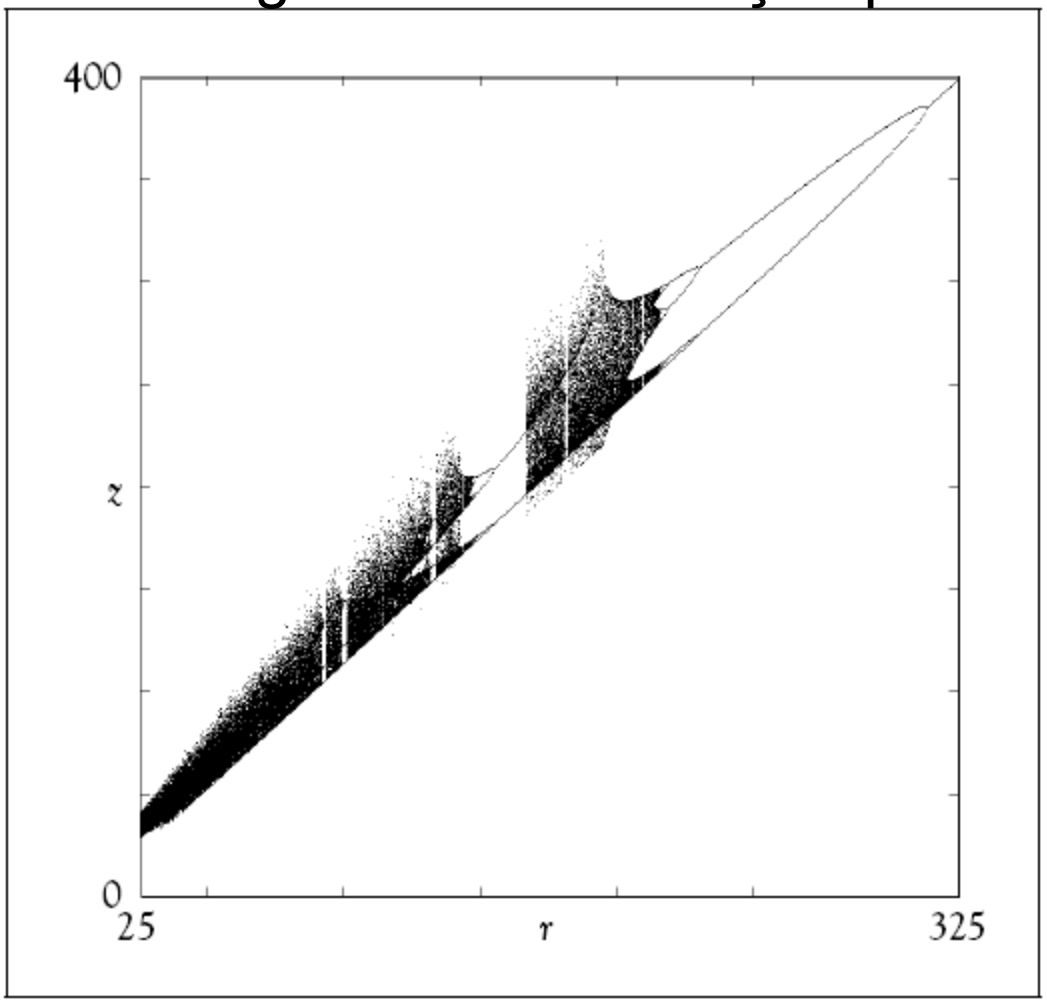

Figure 9.4 Bifurcation diagram of the Lorenz tent map.
The asymptotic behavior of the tent map of Figure 9.3 is plotted as a function of the bifurcation parameter r. The points plotted above each r correspond to the z-maxima of the orbit, so that 1 point means a period-T orbit, 2 points correspond to a period-2T orbit, and so on.

Chaos
Alligood et al.

Transiente Caótico no Sistema de Lorenz

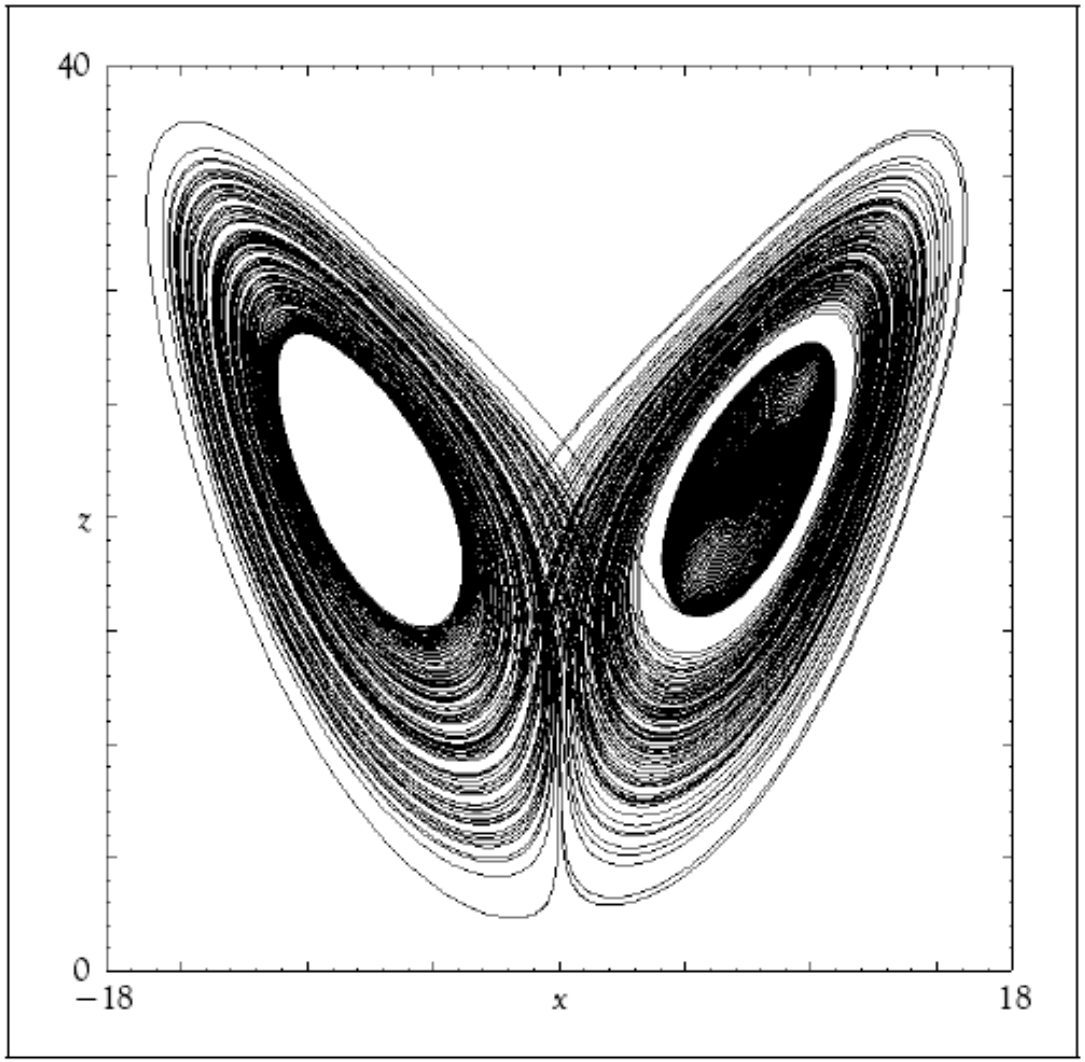

Figure 9.5 Transient chaos in the Lorenz equations.
A trajectory of the Lorenz system has been plotted using $b = 8/3$ and $\sigma = 10$, the same values Lorenz used, but here $r = 23$. When $r < r_1 \approx 24.06$ there is

Chaos
Alligood et al.

Sistema de Roessler

$$\dot{x} = -y - z$$

$$\dot{y} = x + a\,y$$

$$\dot{z} = b + (x - c)\,z$$

Variáveis: $x, y, z \rightarrow$ espaço de fase tridimensional

Parâmetros de controle: $a,\ b,\ c$

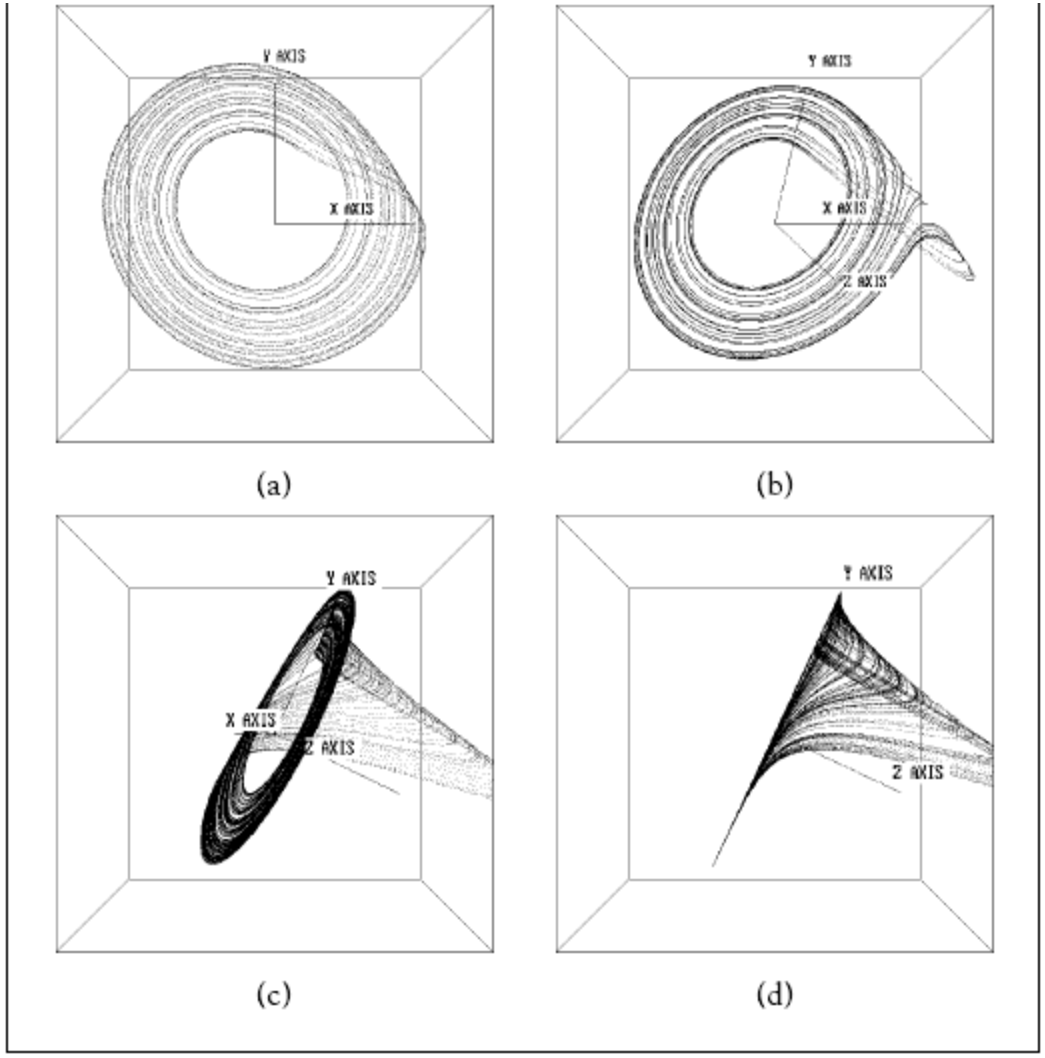

Figure 9.6 The Rössler attractor.
Parameters are set at $a = 0.1$, $b = 0.1$, and $c = 14$. Four different views are shown. The dynamics consists of a spiraling out from the inside along the xy-plane followed by a large excursion in the z-direction, followed by re-insertion to the vicinity of the xy-plane. Part (d) shows a side view. The Lyapunov dimension is 2.005—indeed it looks like a surface.

Atrator Caótico de Roessler

Chaos
Alligood et al.

Atratores do Sistema de Roessler

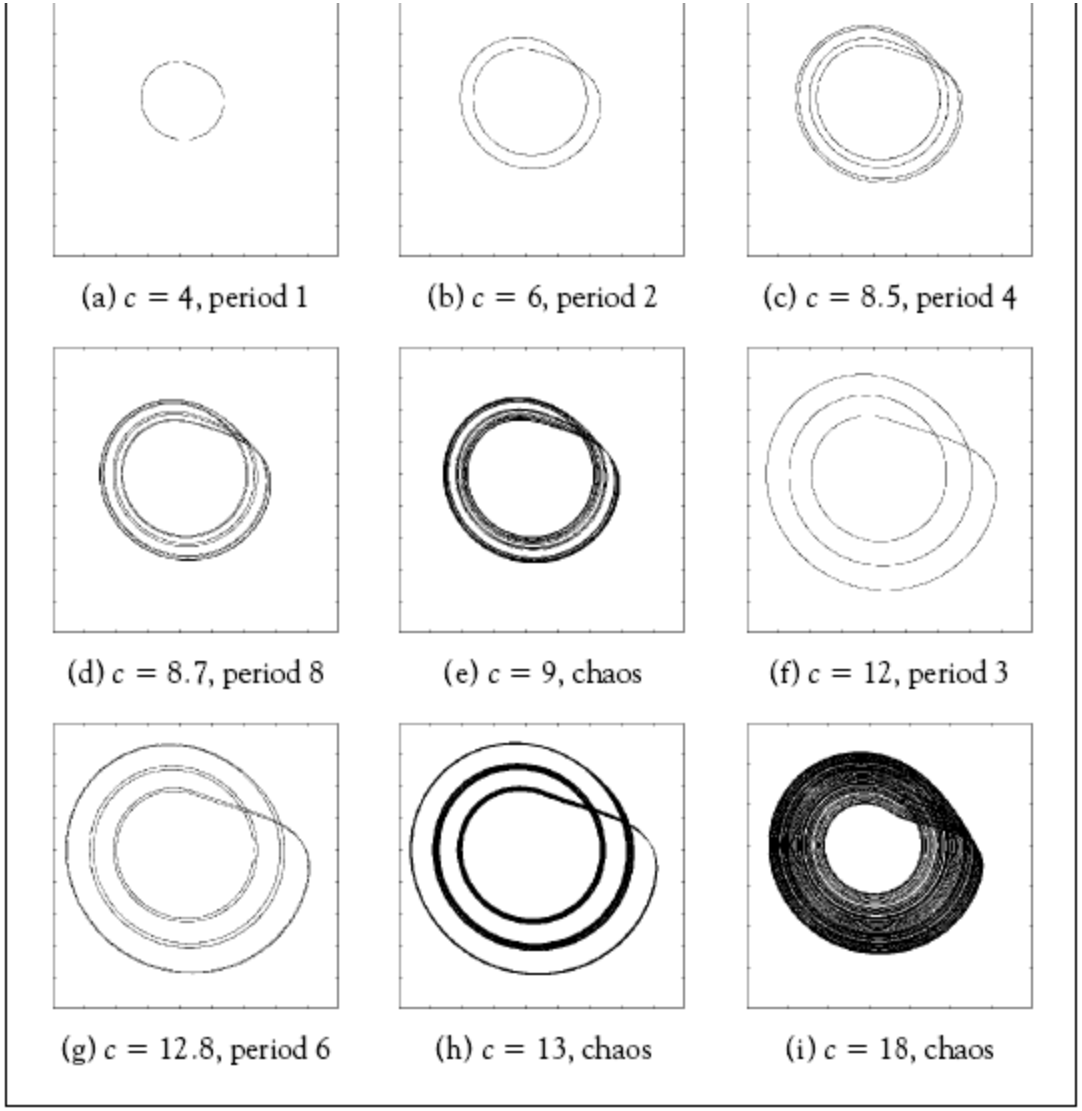

Figure 9.7 Attractors of the Rössler system as c is varied.
Fixed parameters are $a = b = 0.1$. (a) $c = 4$, periodic orbit. (b) $c = 6$, period-doubled orbit. (c) $c = 8.5$, period four. (d) $c = 8.7$, period 8. (e) $c = 9$, thin chaotic attractor. (f) $c = 12$, period three. (g) $c = 12.8$, period six. (h) $c = 13$, chaotic attractor. (i) $c = 18$, filled-out chaotic attractor

Chaos
Alligood et al.

Diagrama de Bifurcação
Sistema de Roessler

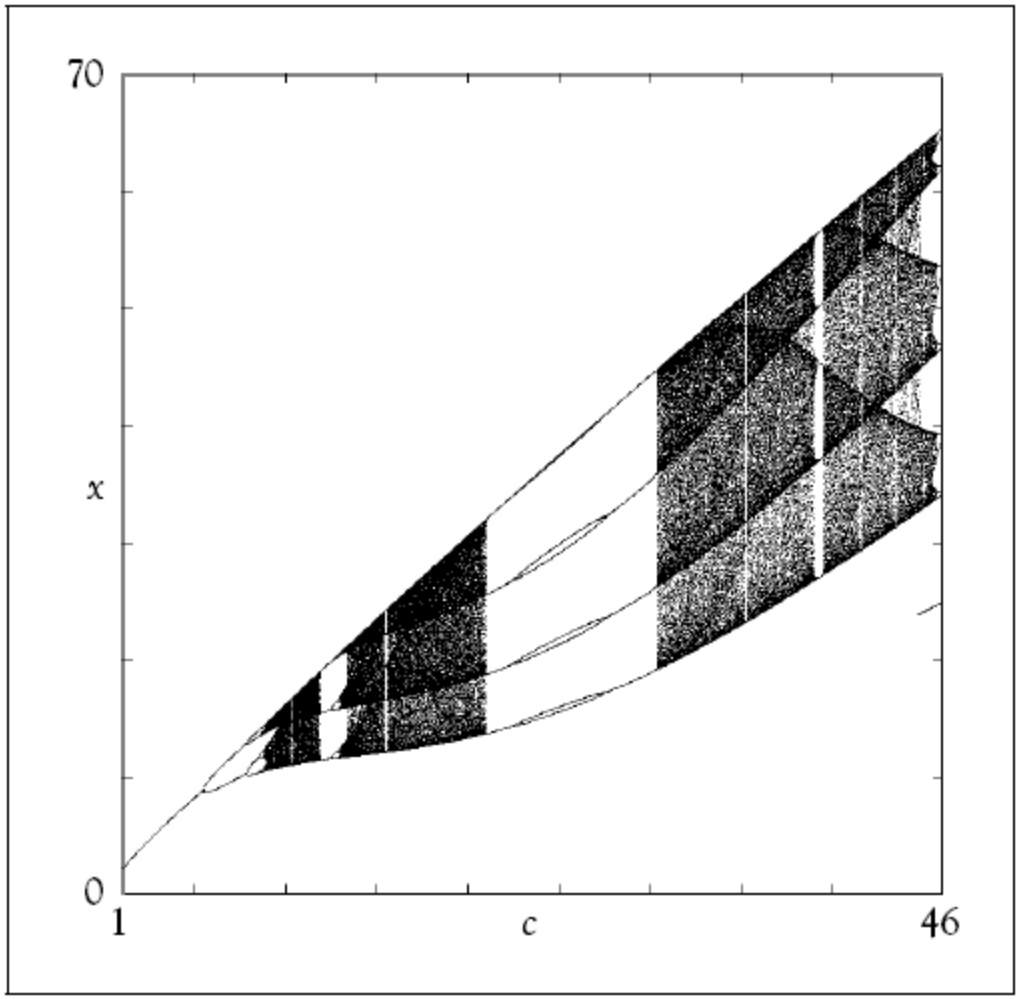

Figure 9.8 Bifurcation diagram for the Rössler equations.
The parameters $a = b = 0.1$ are fixed. The horizontal axis is the bifurcation parameter c. Each vertical slice shows a plot of the local maxima of the x-variable of an attractor for a fixed value of the parameter c. A single point implies there is a periodic orbit; two points mean a periodic orbit with "two loops", the result of a period doubling, and so on. Near $c = 46$ the attractor disappears abruptly.

Chaos
Alligood et al.

The forced damped double-well Duffing equation

$$\ddot{x} + c\dot{x} - x + x^3 = \rho \sin t \tag{9.10}$$

is capable of sustained chaotic motion. As a system in the two variables x and $\dot{x}$, it is nonautonomous; the derivative of $y = \dot{x}$ involves time. The usual trick is to declare time as a third variable, yielding the autonomous three-dimensional system

$$\begin{aligned} \dot{x} &= y \\ \dot{y} &= -cy + x - x^3 + \rho \sin t \\ \dot{t} &= 1 \end{aligned} \tag{9.11}$$

Atrator de Pêndulo Forçado

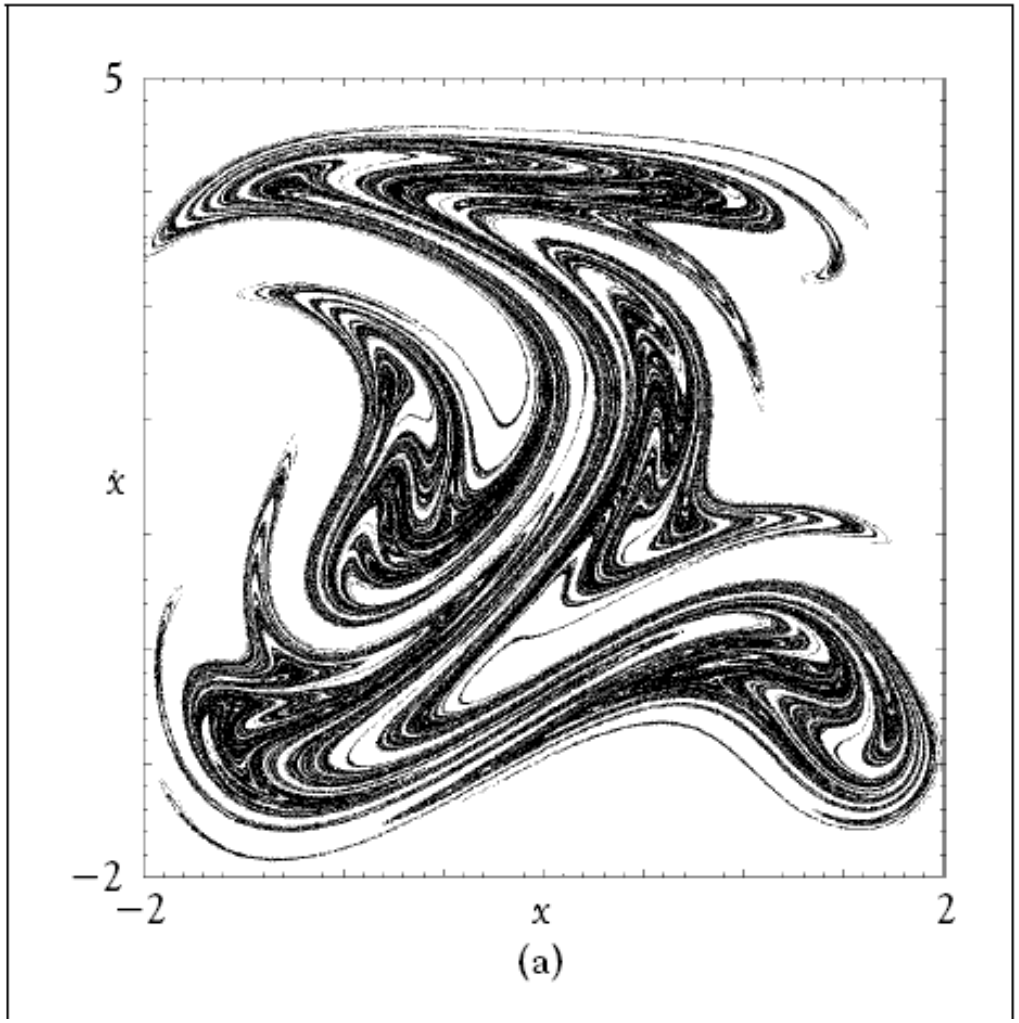

Chaos
Alligood et al.

Mapa Estroboscópico do Atrator da Equação de Duffing

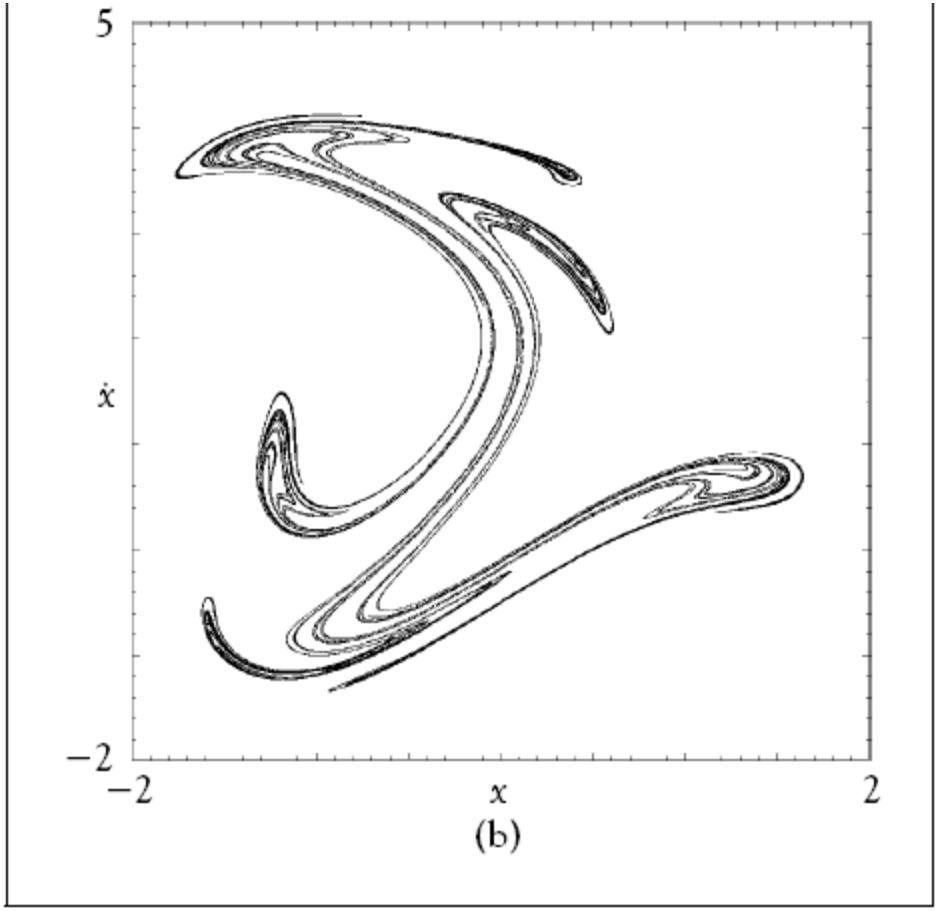

$$\ddot{x} + c\dot{x} - x + x^3 = \rho \sin t$$

Figure 9.11 Time-2π map of the forced damped double-well Duffing equation. (a) The variables $(x, \dot{x})$ of (9.10) with $c = 0.02$, $\rho = 3$ are plotted each 2π time units. One million points are shown. (b) Same as (a), but $c = 0.1$. Compare with Figure 5.24, which was measured from experiment with a qualitatively similar system.

Chaos
Alligood et al.

Mapa Estroboscópico

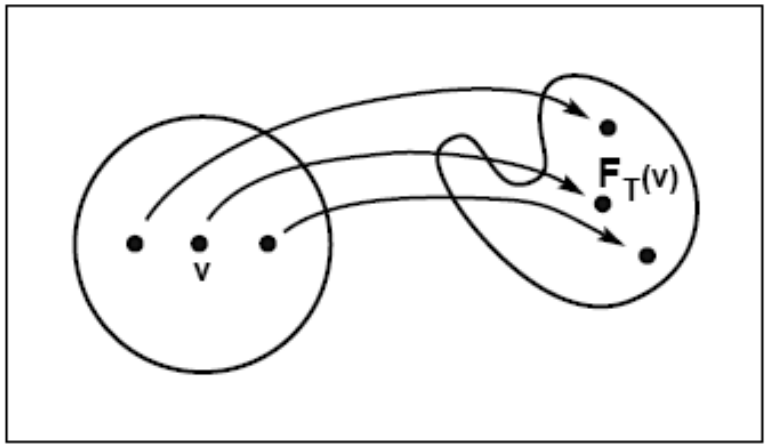

Figure 9.12 The time-T map F_T of a flow.
A ball of initial conditions are followed from time $t = 0$ to time $t = T$. The image of the point $\mathbf{v}$ under F_T is the position of the solution at time T of the initial value problem with $\mathbf{v}_0 = \mathbf{v}$.

Caos no Circuito Elétrico de Chua

Parâmetros de Controle

Controle das Oscilações

Atratores

- M. S. Batista e I. L. Caldas - Physica D (1999).
- R. O. Medrano-T., M. S. Batista e I. L. Caldas, Physica D (2003).

Circuito de Chua

R elemento linear por partes

- Variáveis dinâmicas:
  V_{c1} tensão
  V_{c2} tensão
  i_L corrente

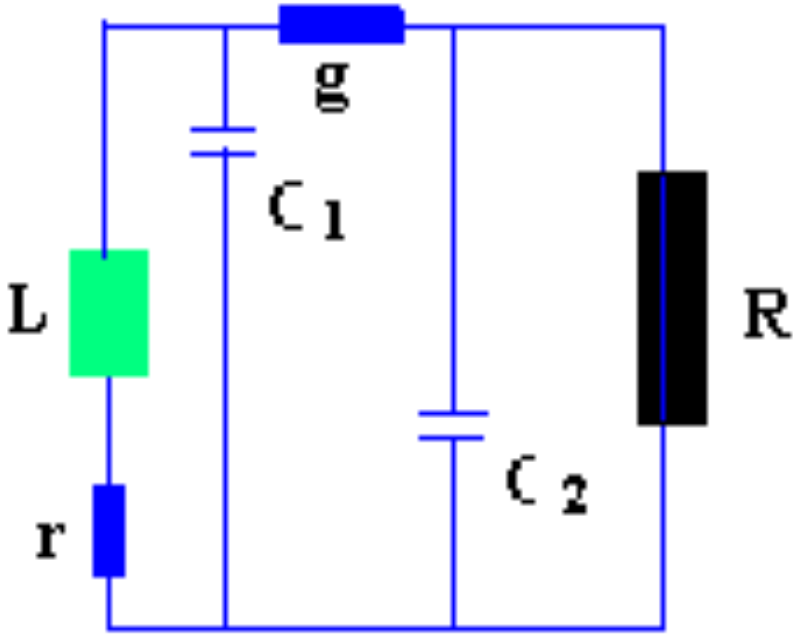

Circuito de Chua

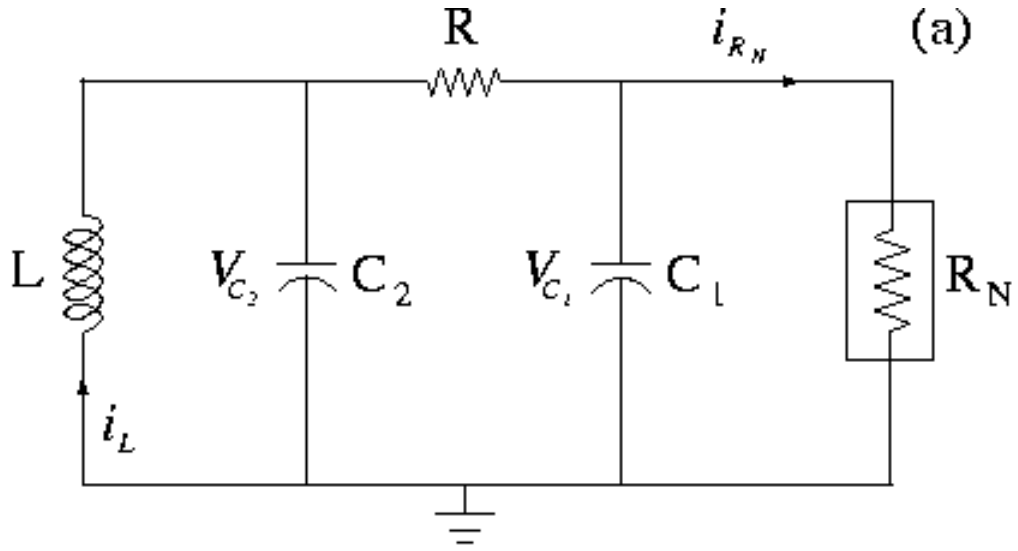

Curva Característica

Linear por partes

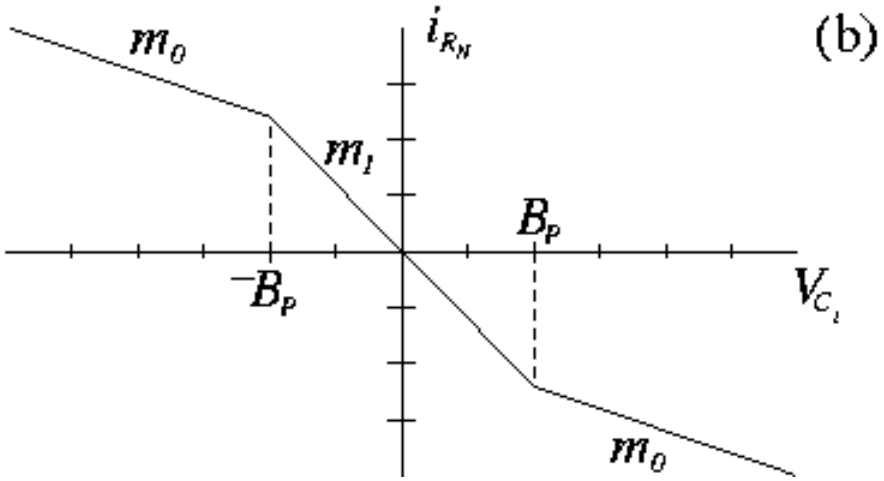

Experiment

Periodic Attractor

V_{c1} voltage across C_1

V_{c2} voltage across C_2

i_L current trough L

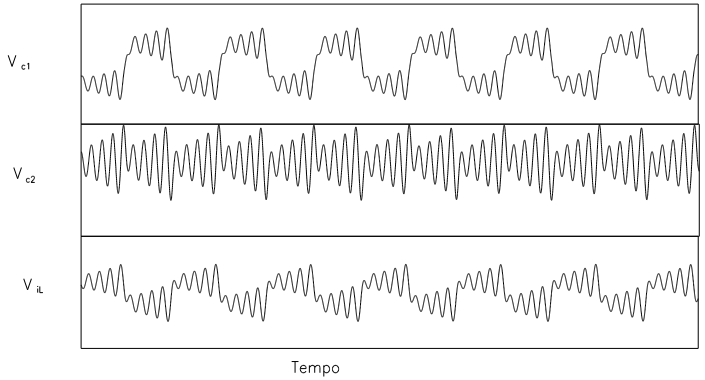

Experiment

- Double Scroll Atrator

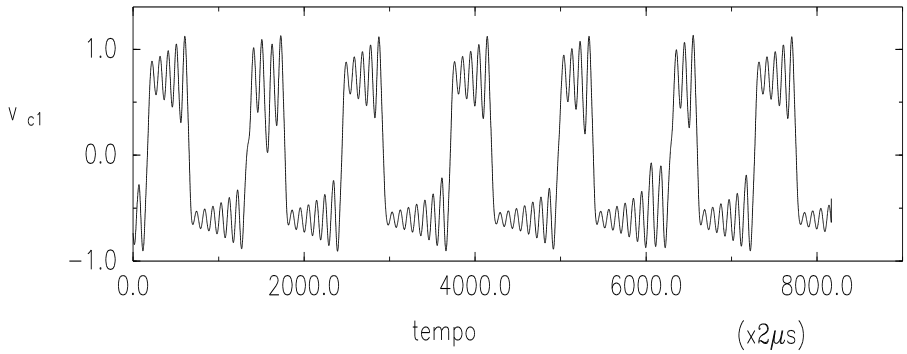

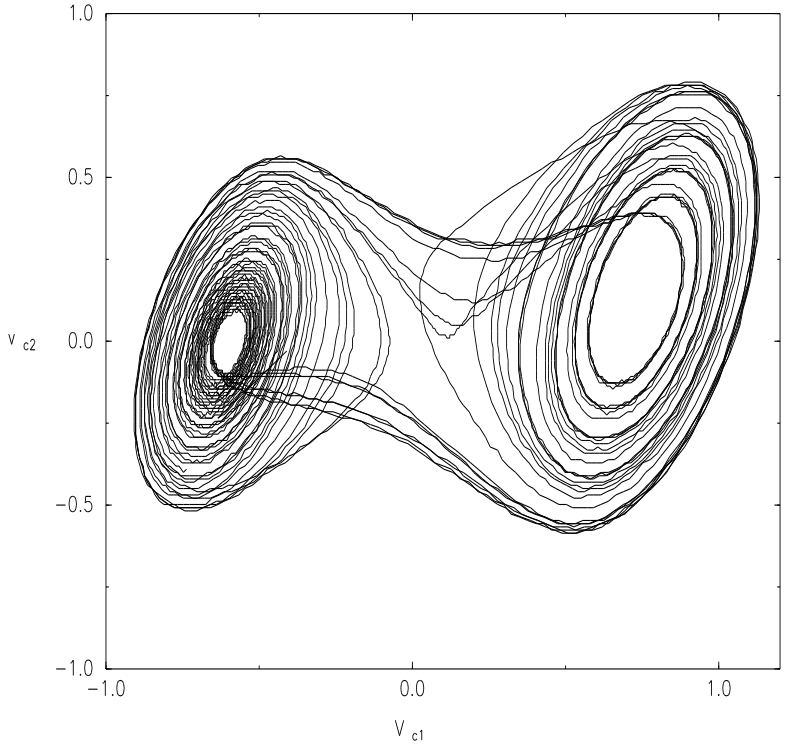

O Circuito de Chua

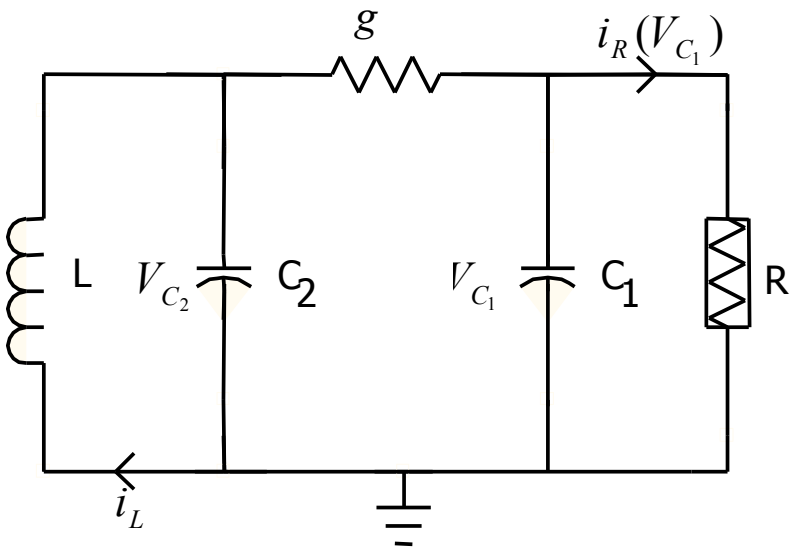

Fig.1. Circuito de Chua. R é a resistência não linear.

Aplicando a lei de Kirchoff ao circuito:

$$C_1\dot{V}_{C_1} = g\left(V_{C_2} - V_{C_1}\right) - i_R\left(V_{C_1}\right)$$
$$C_2\dot{V}_{C_2} = g\left(V_{C_1} - V_{C_2}\right) + i_L$$
$$L\dot{i}_L = -V_{C_2}$$

Simetria ímpar: f(x)=-f(-x)

Resistência Linear por Partes

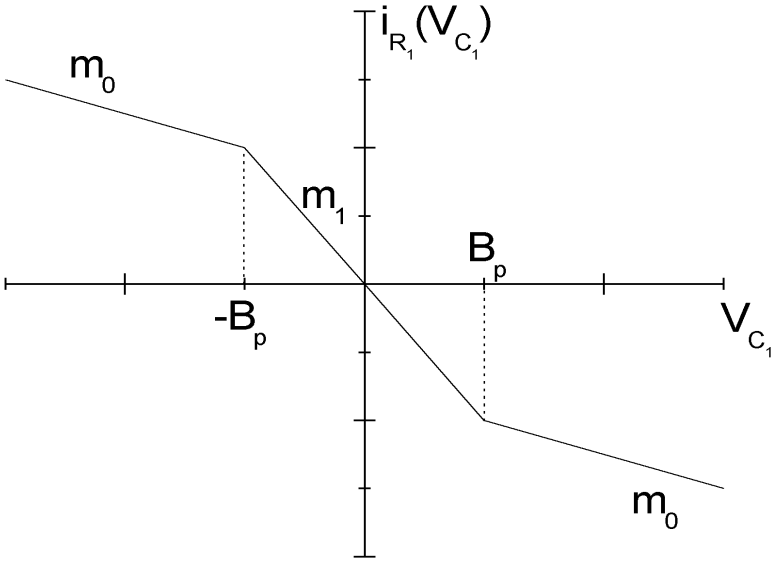

Fig. 2. Curva característica da resistência linear por partes.

Função da curva característica da resistência linear por partes:

$$i_R\left(V_{C_1}\right)=\begin{cases} m_0 V_{C_1}+(m_1-m_0)B_p, & V_{C_1}\geq B_p \\ m_1 V_{C_1}, & \left|V_{C_1}\right|\leq B_p \\ m_0 V_{C_1}-(m_1-m_0)B_p, & V_{C_1}\leq -B_p \end{cases}$$

Sistema Adimensional

Mudança de variáveis:

$$x = \frac{V_{C_1}}{B_p}, \qquad y = \frac{V_{C_2}}{B_p} \quad e \quad z = \frac{i_L}{gB_p}$$

$$\alpha = \frac{C_2}{C_1}, \qquad \beta = \frac{C_2}{g^2 L}, \qquad \tau = \frac{g}{C_2}t,$$

$$a = \frac{m_1}{g} \quad \text{e} \quad b = \frac{m_0}{g}$$

$$\begin{aligned} C_1\dot{V}_{C_1} &= g\left(V_{C_2} - V_{C_1}\right) - i_R\left(V_{C_1}\right) \\ C_2\dot{V}_{C_2} &= g\left(V_{C_1} - V_{C_2}\right) + i_L \\ L\dot{i}_L &= -V_{C_2} \end{aligned}$$

$$\begin{aligned} \dot{x} &= \alpha\left[y - x - k(x)\right] \\ \dot{y} &= x - y + z \\ \dot{z} &= -\beta y \end{aligned}$$

$$i_R\left(V_{C_1}\right) = \begin{cases} m_0 V_{C_1} + (m_1 - m_0)B_p, & V_{C_1} \geq B_p \\ m_1 V_{C_1}, & \left|V_{C_1}\right| \leq B_p \\ m_0 V_{C_1} - (m_1 - m_0)B_p, & V_{C_1} \leq -B_p \end{cases}$$

$$k(x) = \begin{cases} bx + (a-b), & x \geq 1 \\ ax, & |x| \leq 1 \\ bx - (a-b), & x \leq -1 \end{cases}$$

Atratores do Sistema

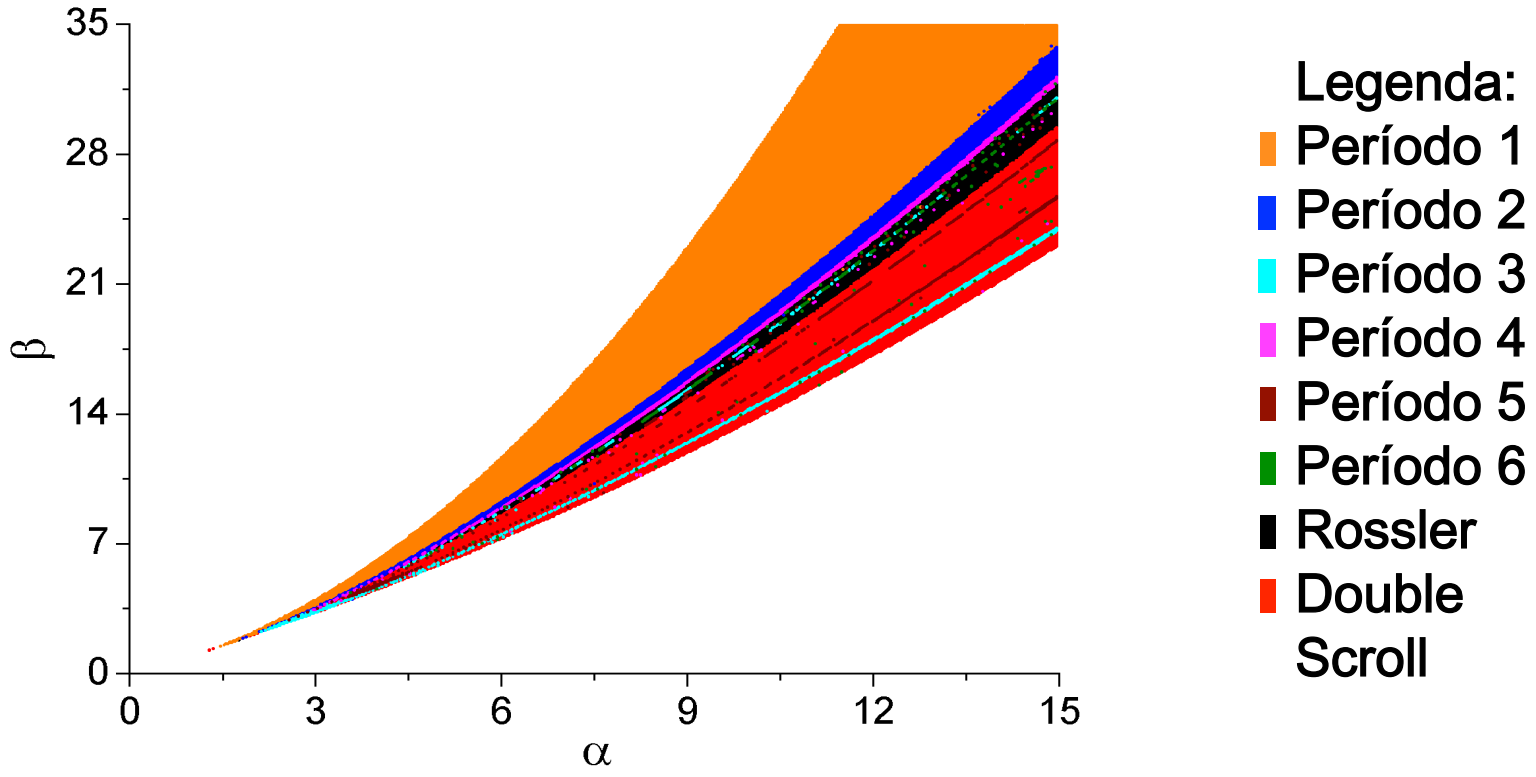

Fig. 3. Atratores no espaço dos parâmetros.

Atratores no Espaço dos Parâmetros

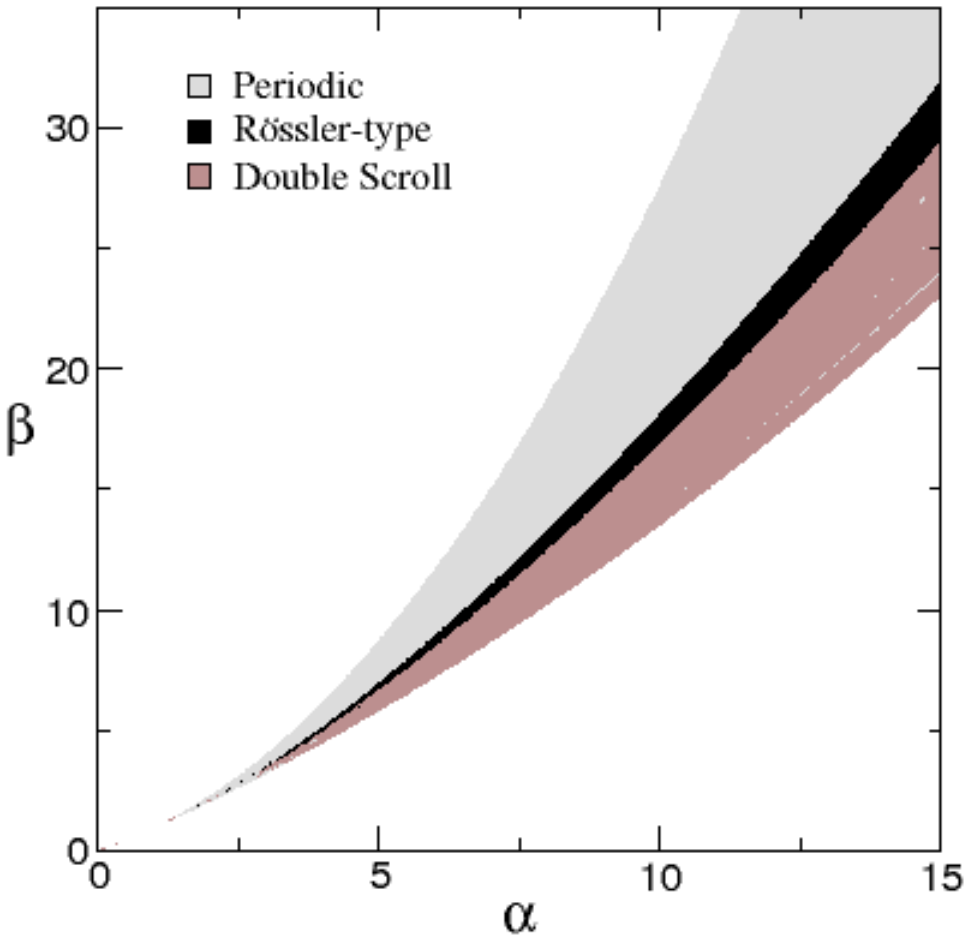

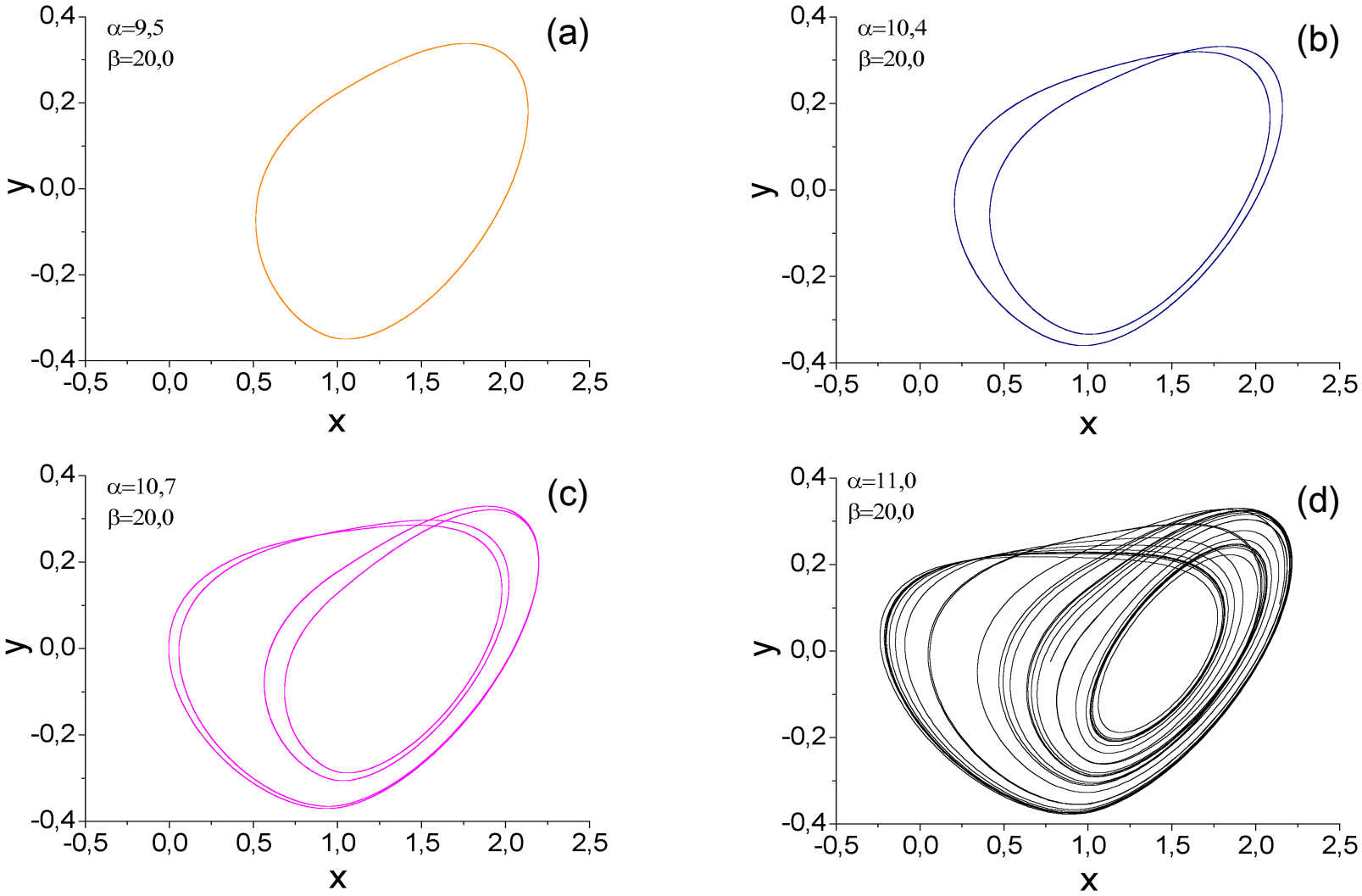

Fig. 4. Atratores: (a) Período 1, (b) Período 2, (c) Período 4, (d) Tipo Rössler.

Atratores do Circuito de Chua

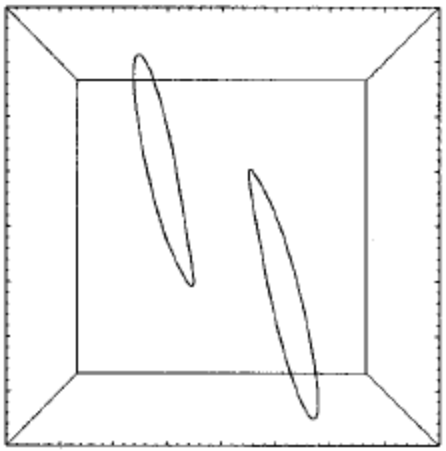

(a) $c_3 = 50$, period 1

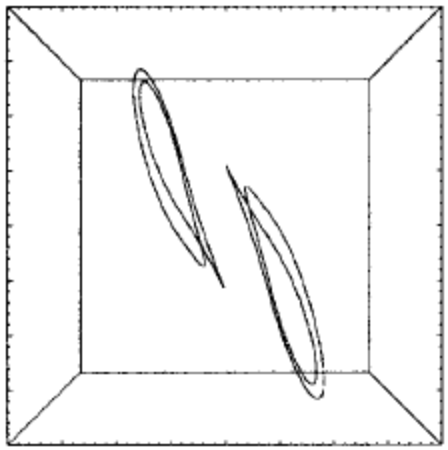

(b) $c_3 = 35$, period 2

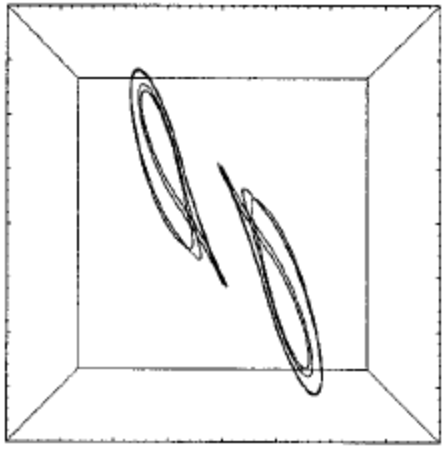

(c) $c_3 = 33.8$, period 4

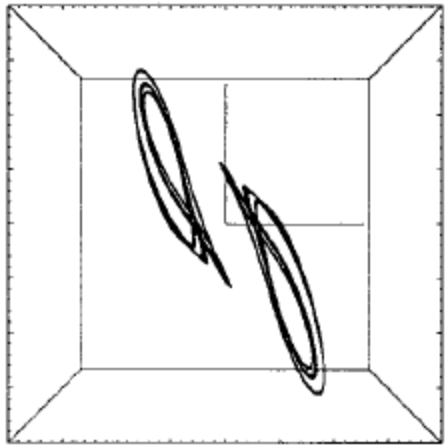

(d) $c_3 = 33.6$, chaos×2

Chaos
Alligood et al.

Atratores do Circuito de Chua

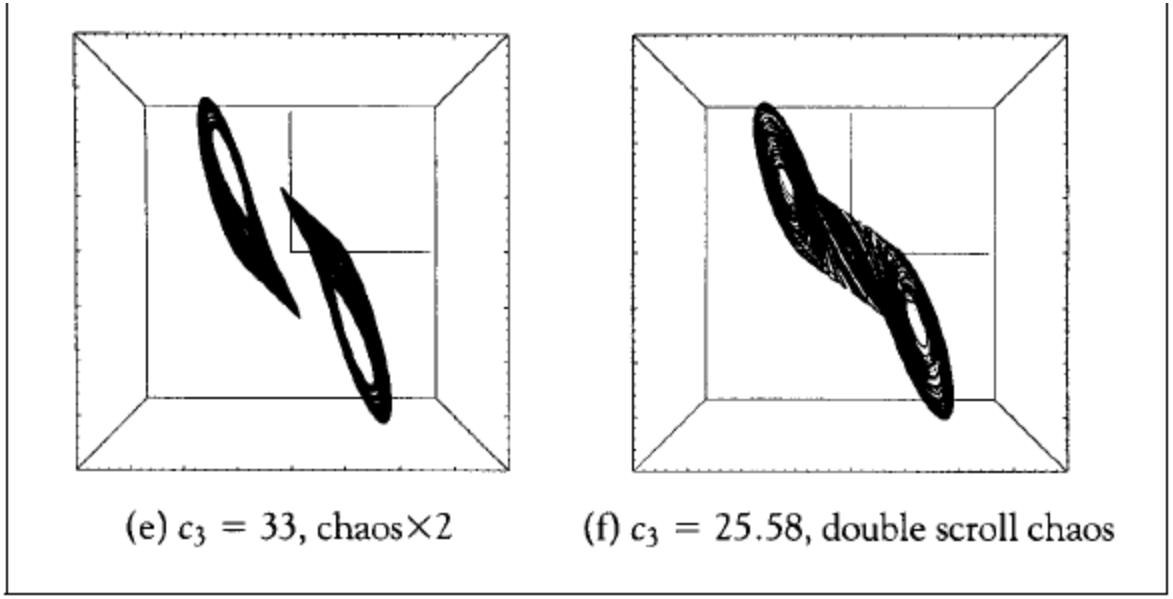

Figure 9.10 Chua circuit attracting sets.
Fixed parameters are $c_1 = 15.6$, $c_2 = 1$, $m_0 = -8/7$, $m_1 = -5/7$. The attracting set changes as parameter c_3 changes. (a) $c_3 = 50$, two periodic orbits. (b) $c_3 = 35$, the orbits have "period-doubled". (c) $c_3 = 33.8$, another doubling of the period. (d) $c_3 = 33.6$, a pair of chaotic attracting orbits. (e) $c_3 = 33$, the chaotic attractors fatten and move toward one another. (f) $c_3 = 25.58$, a "double scroll" chaotic attractor. This attractor is shown in color in Color Plate 18.

Chua
Alligood et al.

Atratores
e
pontos fixos
instáveis

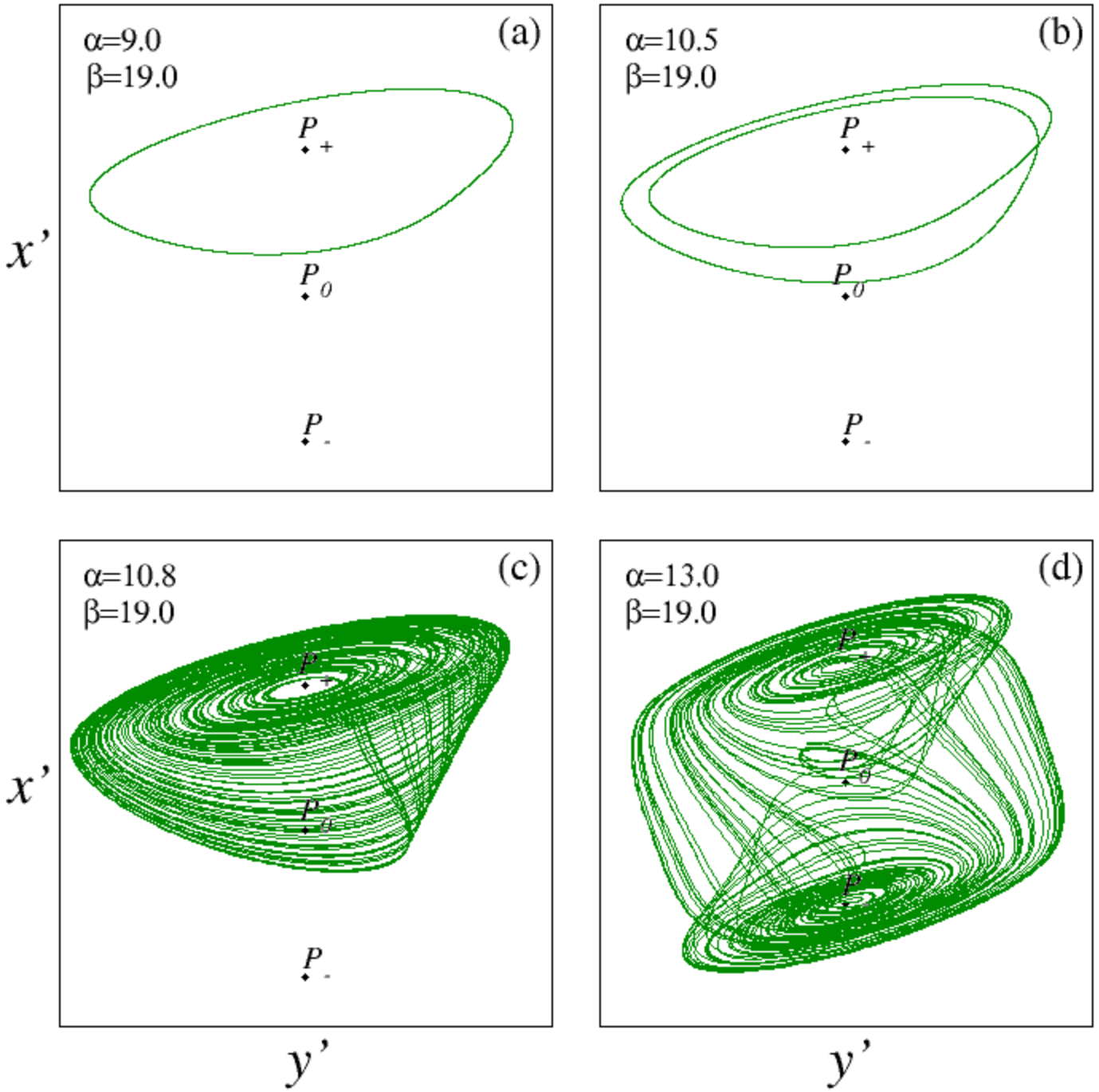

Coexistência de Atratores Caóticos no Circuito de Chua

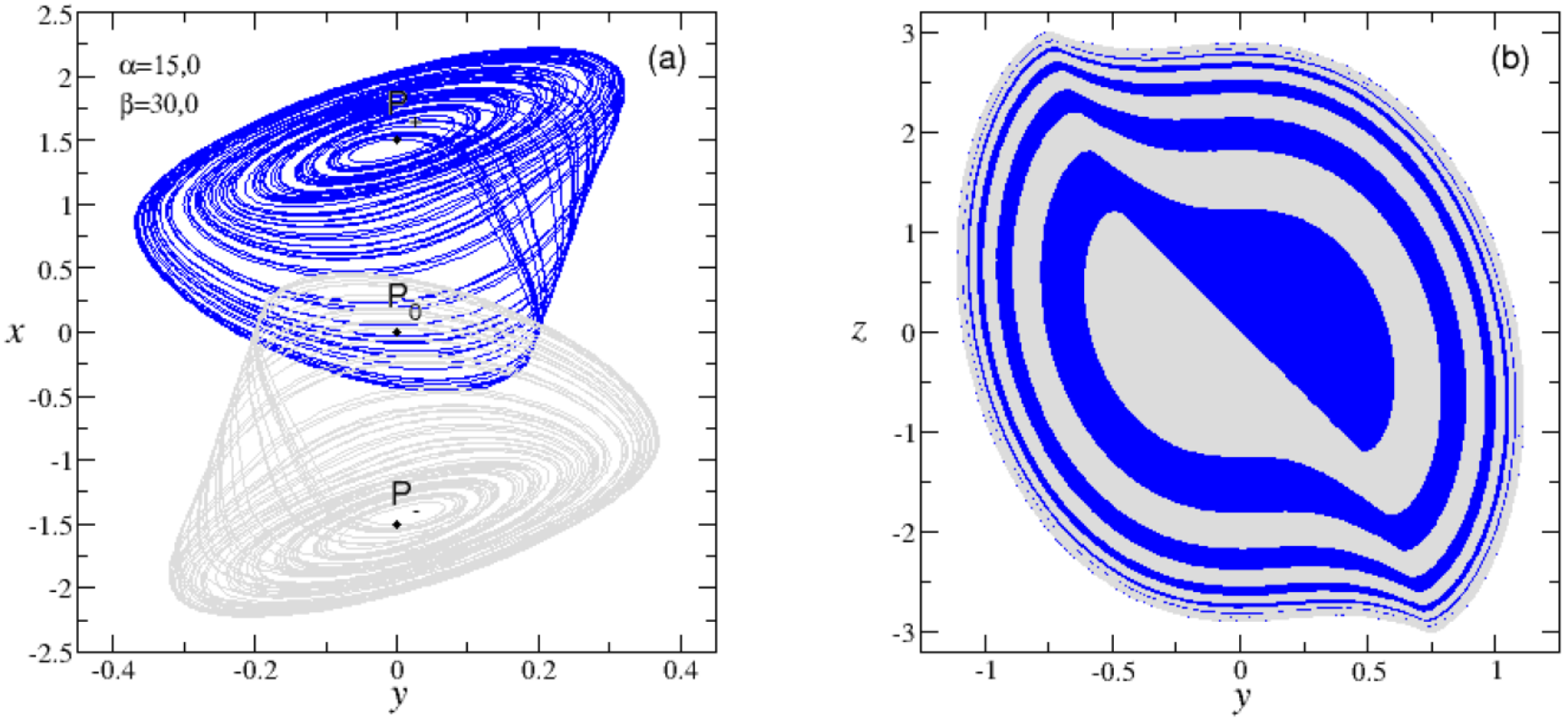

(a) Atratores coexistentes do tipo Rössler (b) Bacia de atração dos atratores em $x = 0$.

Órbita Homoclínica do Circuito de Chua

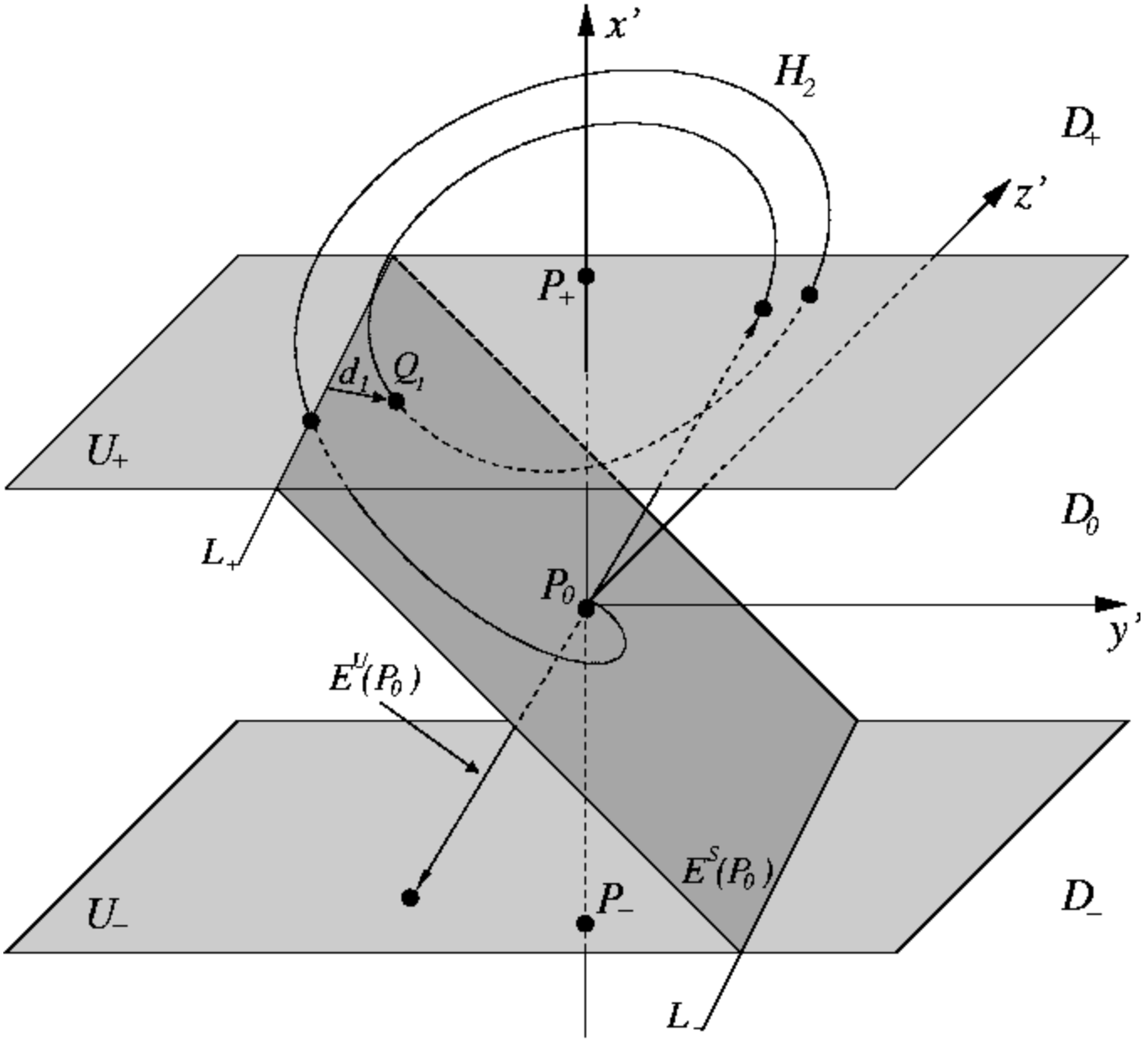

Órbitas Homoclínicas

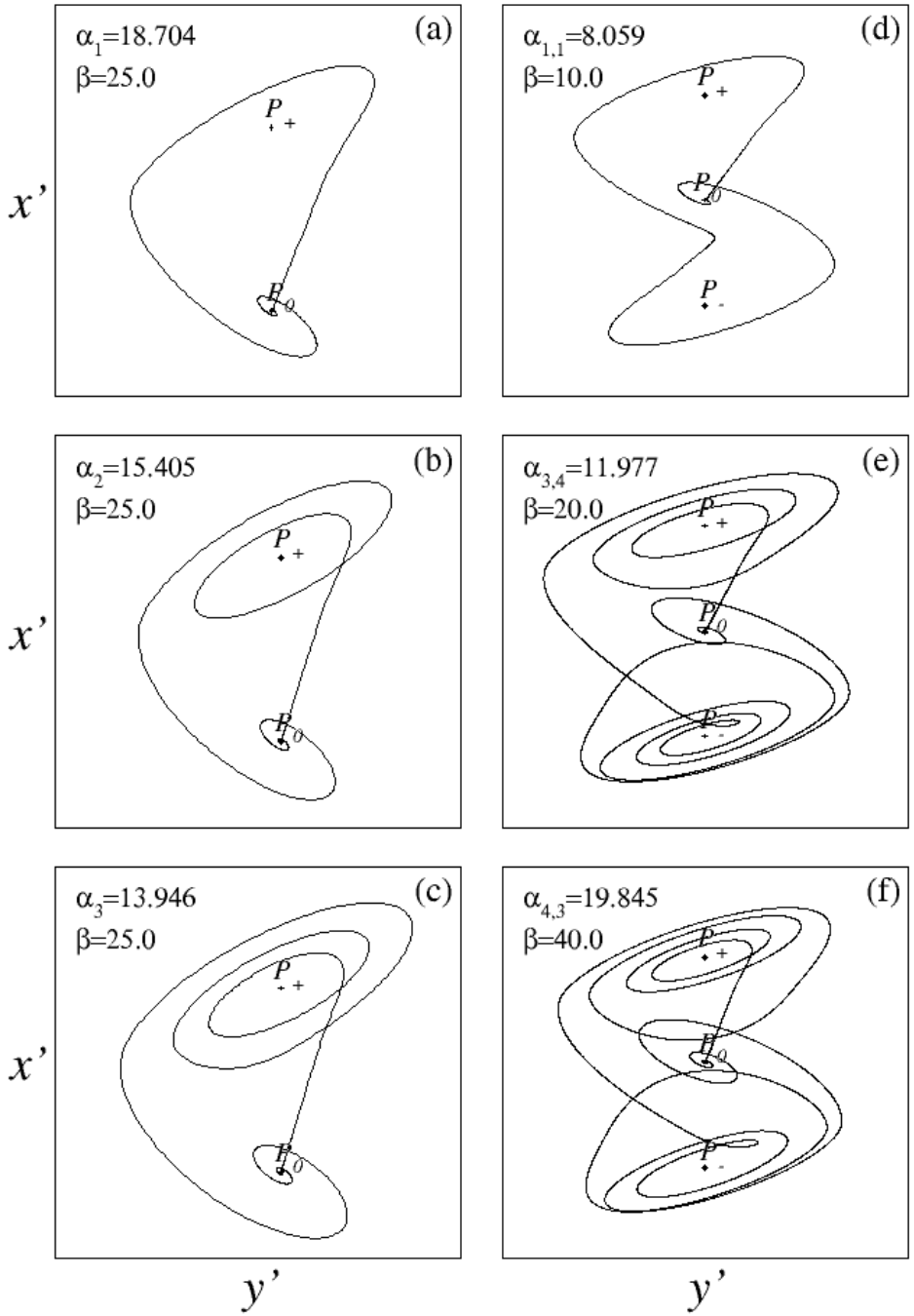

Órbitas Homoclínicas
Espaço dos Parâmetros

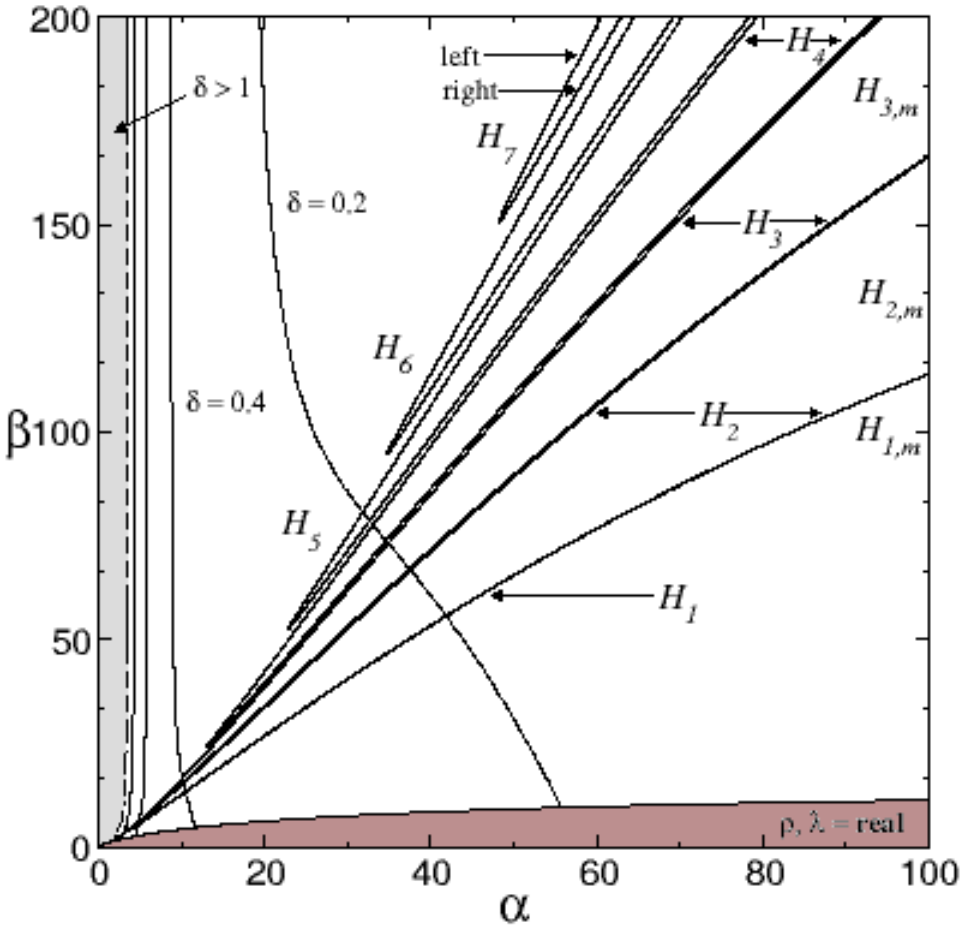

Família de Órbitas Hoclínicas
Espaço dos Parâmetros

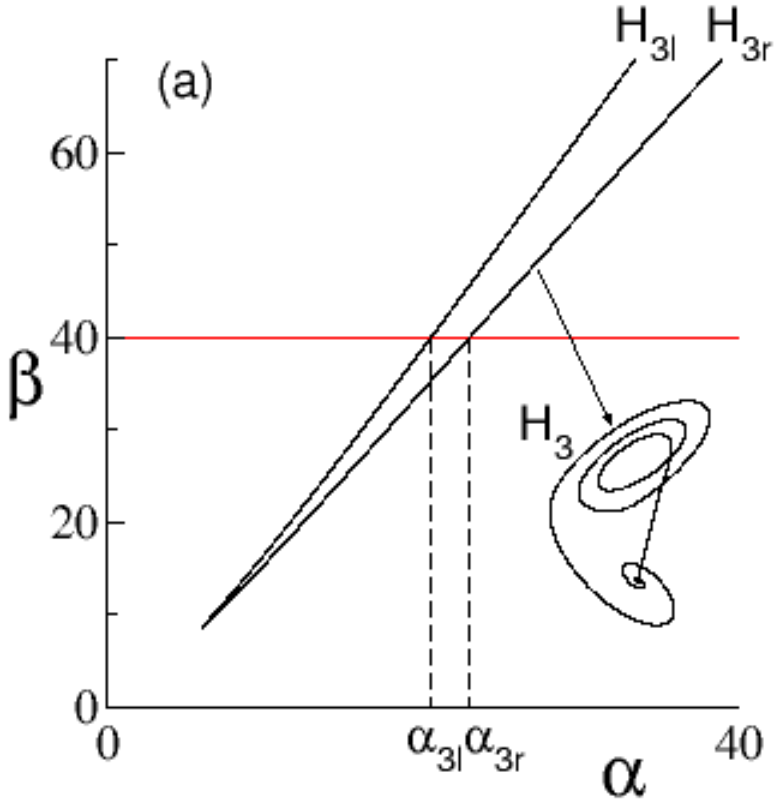

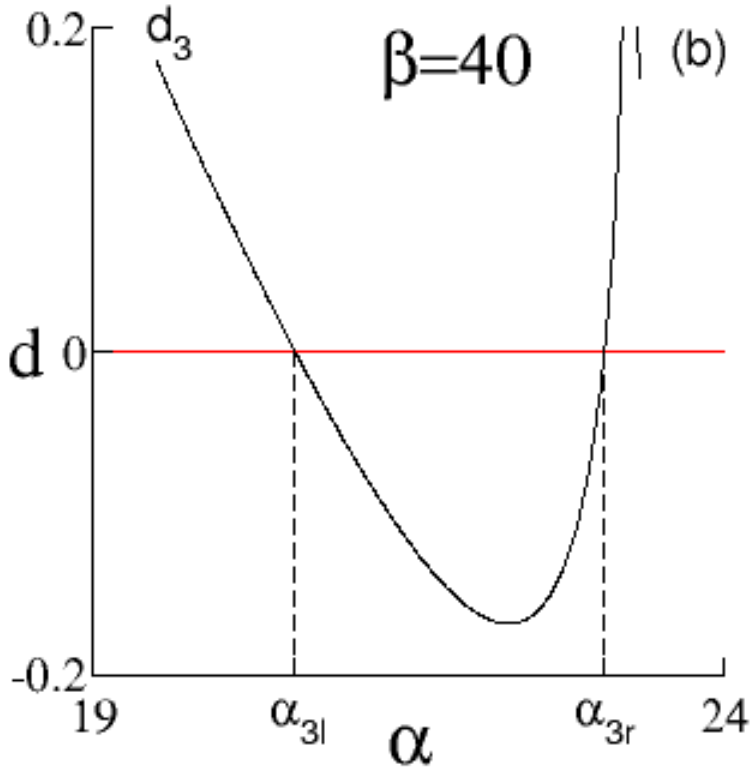

Circuito de Chua Perturbado

Oscilação forçada

Sincronização de dois circuitos

Perturbação Senoidal

(Tese de doutoramento, Murilo Baptista, IF-USP, 1996)

Amplitude = 14Volts

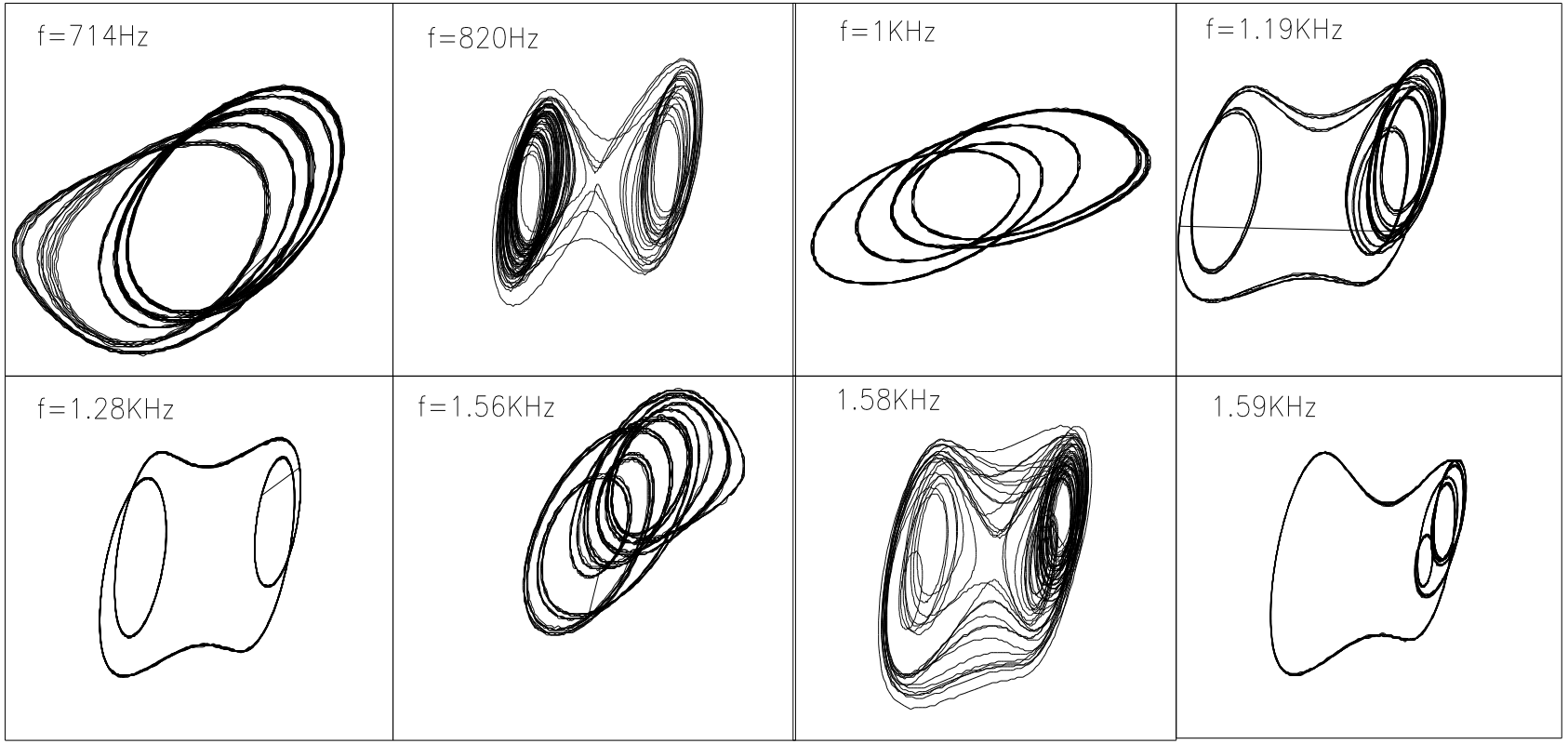

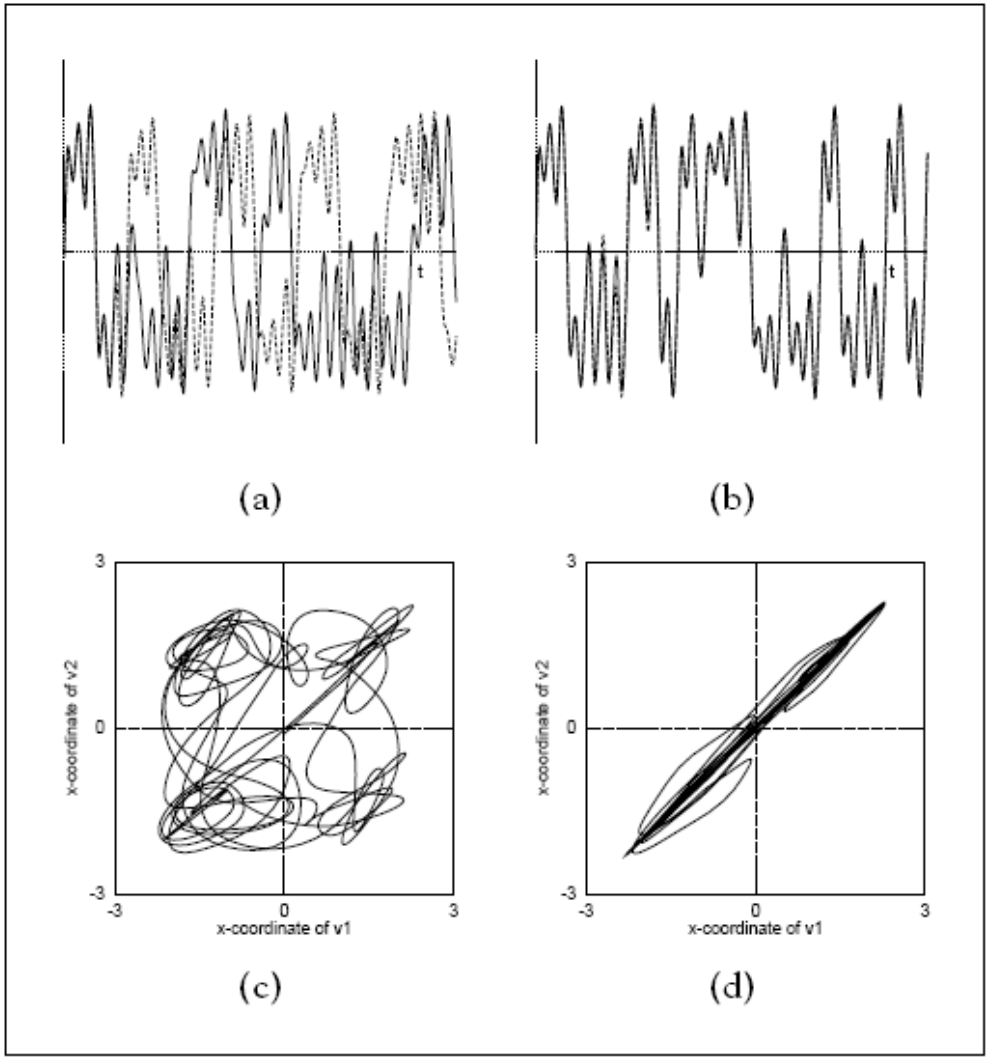

Sincronização de Dois circuitos de Chua

(tese de doutoramento
Elinei dos Santos
IF-USP, 2001)

Figure 9.14 Synchronization of the Chua attractor.
(a) Time traces of the x-coordinates of $\mathbf{v}_1$ (solid) and $\mathbf{v}_2$ (dashed) for coupling strength $c = 0.15$. (b) Same as (a), but for $c = 0.30$. (c) A simultaneous plot of one curve from (a) versus the other shows a lack of synchronization. (d) Same as (c), but using the two curves from (b). The plot lines up along the diagonal since the trajectories are synchronized.

Chaos
Alligood et al.